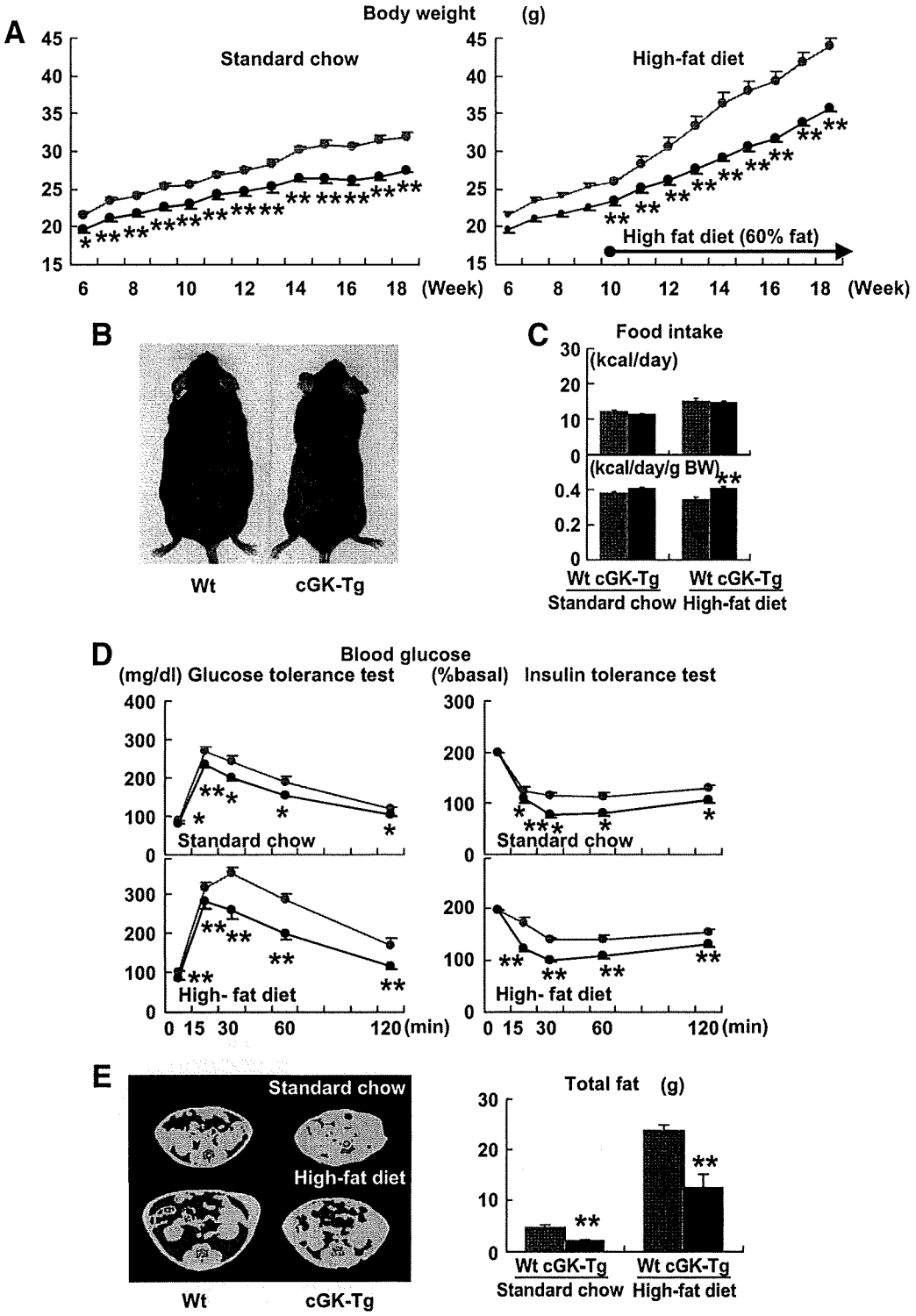

FIG. 4. cGK-Tg mice are lean and insulin sensitive even on standard diet. Wild-type and cGK-Tg mice were given a high-fat (60 kcal% fat) diet from the age of 10 weeks. *A*: Body weight of cGK-Tg mice on standard diet (*left panel*) and high-fat diet (*right panel*) (n = 8–10). ▤, wild type; ■, cGK-Tg. *B*: Macroscopic appearance of a wild-type (Wt) and a cGK-Tg mouse. *C*: Food intake on standard and high-fat diet (*upper panel*) (kcal/day, n = 6) and the body weight (BW)-adjusted value (*lower panel*) (kcal · day^{-1} · g body wt^{-1}). *D*: Blood glucose levels determined with the glucose and insulin tolerance tests for each genotype on standard diet and high-fat diet (n = 8). ▤, wild type; ■, cGK-Tg. *E*: CT images obtained at kidney level of a wild-type (Wt) and a cGK-Tg mouse on standard diet (*upper panel*) and high-fat diet (*lower panel*). Subcutaneous fat (yellow), abdominal fat (red), and muscular region (blue) were distinguished. Total fat weight was estimated from the images (n = 6). *F*: Microscopic analysis using hematoxylin and eosin staining of epididymal fats in high-fat–fed mice. Scale bar, 100 μm. *G*: Distribution of adipocyte diameter determined with Coulter counter (n = 8). ▤, wild type; ■, cGK-Tg. *H*: Macroscopic appearance of the liver in high-fat–fed mice (*upper panel*). Microscopic images with Oil red O staining of the liver (*lower panel*). Scale bar, 100 μm. *I* and *J*: Triglyceride concentration in the liver (*I*) and the quadriceps (*J*) (n = 12). *P < 0.05; **P < 0.01 vs. wild type on the same feeding condition. (A high-quality color digital representation of this figure is available in the online issue.)

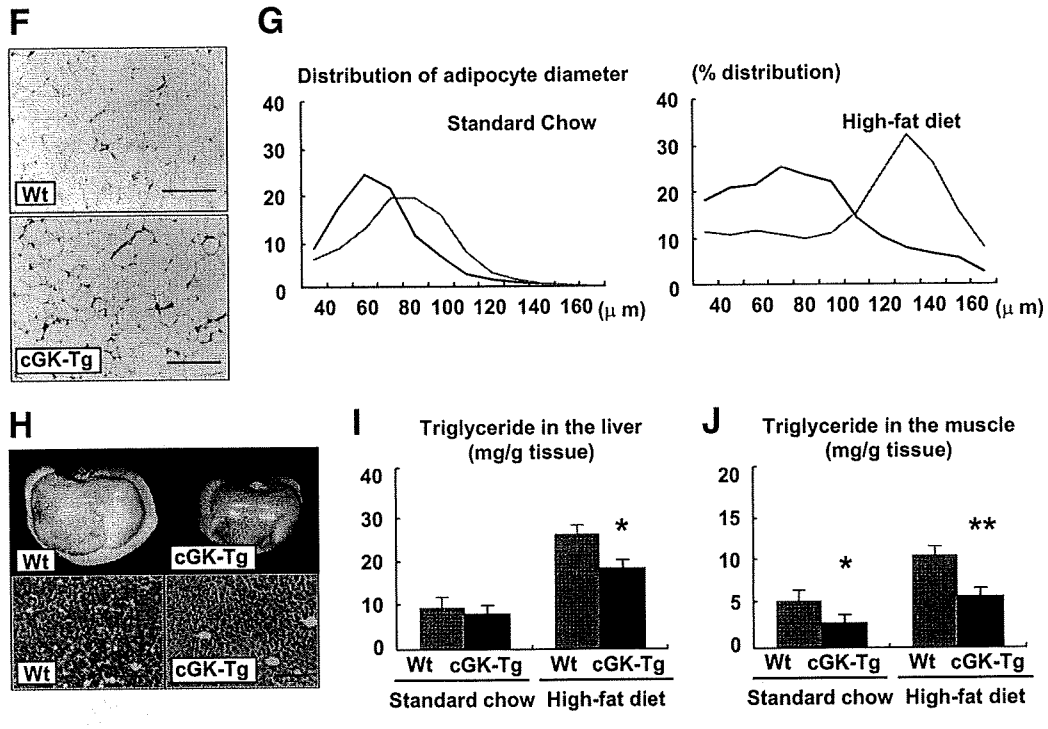

FIG. 4. Continued.

increase in their downstream target genes involved in mitochondrial oxidative function and fatty acid catabolism (Fig. 5*H*). In addition to PGC-1α and PPARδ, the expression of ATP synthase (ATPsyn), cythochrome c oxidase (COX), and carnitine palmitoyl transferase (CPT) 1b was significantly enhanced in the skeletal muscle of cGK-Tg mice, compared with wild-type mice, both when on standard diet and high-fat diet; while UCP3, fatty acid transporter (FATP), and acyl-CoA oxidase (ACO) were upregulated when on the high-fat diet only (Fig. 5*H*). The expression of PPARα in the skeletal muscle of cGK-Tg mice was not significantly different from wild-type mice, although high-fat diet increased the expression (data not shown). Giant mitochondria were densely packed in the skeletal muscle of high-fat–fed cGK-Tg mice when it was observed by means of an electron microscope (Fig. 5*I*).

NPs directly increase the expression of PGC-1α and PPARδ and mitochondrial content in cultured myocytes. The results of the study shown in Fig. 6*A* and *B* are described in supplement 2. Schematic representation of the suggested roles for NP/cGK cascades, as described in the present and previous studies, is shown in Fig. 6*C*.

TABLE 2
Physical and metabolic parameters of cGK-Tg mice fed on standard chow or high-fat diet

	Standard chow		High-fat diet	
	Wild type	cGK-Tg	Wild type	cGK-Tg
Body weight (g)				
18 weeks old	32.0 ± 0.6	27.6 ± 0.4*	43.9 ± 1.2	35.7 ± 1.4*
Glucose (mg/dl)				
Ad libitum feeding	160.7 ± 6.0	137.7 ± 5.1*	233.5 ± 17.1	174.0 ± 7.7*
24-h fasting	93.5 ± 4.7	78.8 ± 2.3†	113.5 ± 7.6	89.8 ± 3.7†
Insulin (ng/dl)				
Ad libitum feeding	1.4 ± 0.2	0.8 ± 0.2†	9.1 ± 1.0	3.5 ± 0.6*
24-h fasting	0.26 ± 0.05	0.23 ± 0.03	0.95 ± 0.22	0.41 ± 0.05†
Triglyceride (mg/dl)				
Ad libitum feeding	103.3 ± 10.1	89.2 ± 7.0	134.9 ± 11.5	134.9 ± 15.8
24-h fasting	84.3 ± 6.8	81.6 ± 6.9	112.8 ± 9.5	103.4 ± 11.6
Fatty acid (mEq/l)				
Ad libitum feeding	1.04 ± 0.05	0.84 ± 0.10	1.32 ± 0.18	1.08 ± 0.11
24-h fasting	1.69 ± 0.09	1.86 ± 0.08	1.66 ± 0.09	2.22 ± 0.08*
Epinephrine (ng/day)				
Urinary excretion	48.2 ± 9.3	52.7 ± 12.8	49.6 ± 6.3	40.5 ± 6.1
Norepinephrine (ng/day)				
Urinary excretion	312.3 ± 62.2	312.3 ± 97.4	547.7 ± 62.2	570.3 ± 47.6

*$P < 0.01$, †$P < 0.05$ compared with wild type on the same feeding condition.

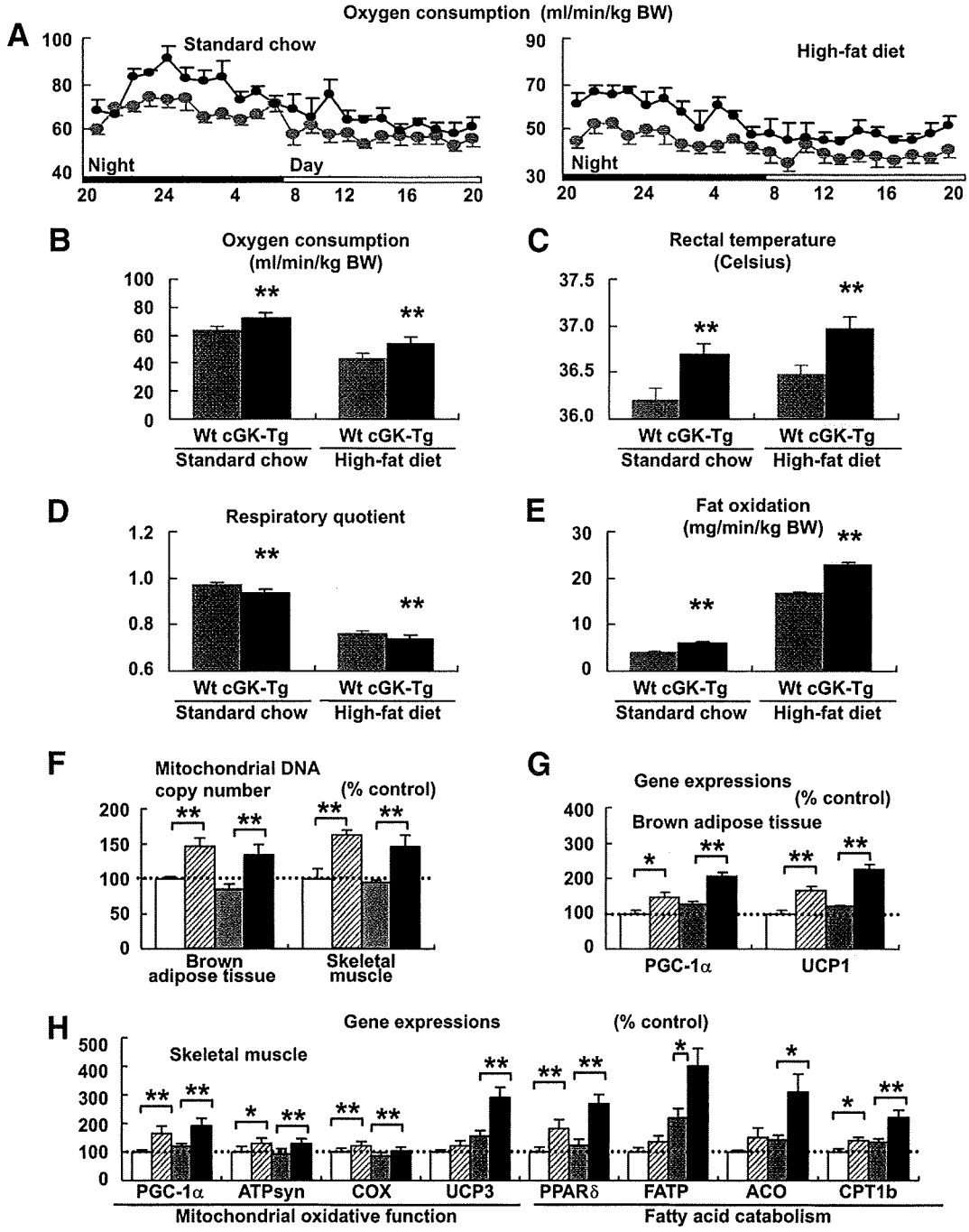

FIG. 5. cGK-Tg mice exhibit giant mitochondria in the skeletal muscle, associated with higher oxygen consumption and fat oxidation. Mice were subjected to respiratory gas analysis after fed on high-fat diet. Total DNA and RNA were extracted from the brown adipose tissue and the quadriceps, and quantitative PCR analysis was performed. *A*: Oxygen consumption on standard diet (n = 6). ▤, wild type; ■, cGK-Tg. *B*: Mean oxygen consumption for 24 h on standard or high-fat diet. *C*: Rectal temperature on standard or high-fat diet (n = 12). *D*: Mean respiratory quotient for 24 h on standard or high-fat diet (n = 6). *E*: Mean fat oxidation estimated from the respiratory gas analysis for 24 h on standard or high-fat diet (n = 6). *F*: Mitochondrial DNA copy number estimated from quantification of mitochondrial and nuclear genome (n = 8). *G*: Expressions of genes encoding PGC-1α and UCP1 in the brown adipose tissue. The values were standardized to those for the control (wild-type [Wt] mice fed on standard diet) in either group (n = 12). *H*: Expressions of the genes involved in mitochondrial regulation or fatty acid catabolism in the skeletal muscle (n = 12). Standard diet: □, wild type (control); ▨, cGK-Tg. High-fat diet: ▤, wild type; ■, cGK-Tg. *I*: Electron microscopic analysis of muscle mitochondria of high-fat–fed cGK-Tg mice. *P < 0.05; **P < 0.01 vs. wild-type mice on the same feeding condition.

DISCUSSION

The findings in this study demonstrate that the activation of NP/cGK cascades augments mitochondrial biogenesis and fat oxidation in mice through upregulation of PGC-1α and PPARδ in the skeletal muscle, thus conferring resistance to obesity and glucose intolerance. BNP-Tg mice fed a high-fat diet were protected from obesity and insulin resistance, while cGK-Tg mice were lean even on standard diet and showed increased insulin sensitivity, and, surprisingly, giant mitochondria were densely packed in the

I

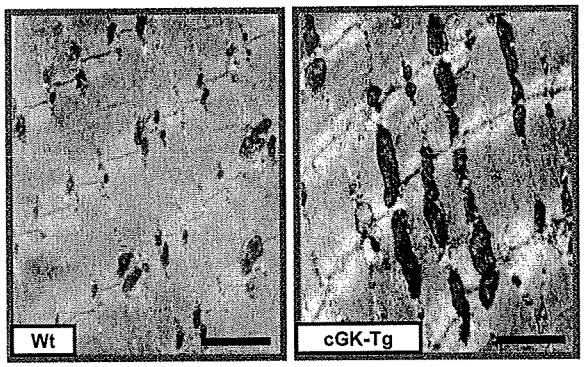

FIG. 5. Continued.

skeletal muscle. Both types of mice showed a reduction in fat tissue and excessive lipid accumulation in the liver and skeletal muscle, in accordance with an increase in fat oxidation. Functional NP receptors were upregulated during fasting, whereas they were downregulated by ad libitum feeding or high-fat challenge, while whole-body knockdown of the functional receptor, GCA, led to promotion of obesity in mice. These findings, together with those that demonstrated NP-induced lipolysis, lead us to propose the concept that NP/cGK cascades play significant roles in lipid catabolism during fasting or chronic caloric restriction, in addition to their well-known roles in the cardiovascular system, such as in the attenuation of hypertension and congestive heart failure (Fig. 6*C*) (7,8,17).

Genetic overexpression of NP/cGK in mice attenuated diet-induced obesity and insulin resistance, associated with the increase in muscle mitochondrial content and fat oxidation. We identified the dual upregulation of PGC-1α and PPARδ in the skeletal muscle of the Tg mice as a molecular basis of the increase in mitochondria and confirmed the direct increase in the expression of PGC-1α and PPARδ and mitochondrial content by both ANP and BNP through the experiments using cultured myocytes. PGC-1α is a transcriptional cofactor that acts as a master regulator of mitochondrial biogenesis (18). PPARδ is a transcription factor that binds with PGC-1α and enhances mitochondrial biogenesis and lipid catabolism (19). Activation of PPARδ in mice by the treatment with the PPARδ agonist GW501516 or overexpression of a constitutively active form of PPARδ were shown to increase muscle mitochondrial content and fatty acid oxidation and, thus, prevent diet-induced obesity and glucose intolerance (20,21). However, mice with muscle-specific overexpression of wild-type PPARδ did not exhibit such a prominent phenotype (22). Muscle-specific overexpression of PGC-1α has been reported to not prevent diet-induced obesity and insulin resistance in mice, although there was an increase in mitochondrial content (23). These results indicate that the coordinated increase in the expression of PGC-1α and PPARδ, which was observed in the skeletal muscle of BNP- and cGK-Tg mice, led to synergistic effects that were beneficial for ameliorating diet-induced obesity and insulin resistance. The expression of PGC-1α and PPARδ in muscle is augmented by exercise via exercise-sensitive molecules such as AMP-activated protein kinase (AMPK) (18,19). The increases in circulating NP and cGMP levels during exercise have been demonstrated in previous reports (24,25). Therefore, we hypothesize that NP/cGMP/cGK cascades can interact with the exercise-sensitive molecules in muscle and increase the expression of PGC-1α and PPARδ.

BNP-Tg mice gained less body weight than controls when they were fed on high-fat diet. The same tendency was observed even when on standard diet; however, the magnitude of the change was not so prominent. We interpret the results as the Tg mice escaped from diet-induced obesity by increasing muscle mitochondrial content and fat oxidation. The elevation of serum adiponectin levels observed in the high-fat–fed BNP-Tg mice, associated with reduced adiposity, might be contributing to the attenuation of insulin resistance (26,27). Apparent changes in food intake and catecholamine kinetics were not observed.

In cGK-Tg mice, the increase in mitochondria was evident even on standard diet, resulting in the Tg mice being leaner and more insulin sensitive than BNP-Tg mice. Our data suggested that one reason for the difference in the magnitude of the altered phenotypes between the BNP- and cGK-Tg mice was caused by the variations of the target tissues. In the skeletal muscle, similar changes in gene expression were evident in the two lines of Tg mice, including upregulation of PGC-1α and PPARδ. In the brown adipose tissue, on the other hand, the increase in the expression level of PGC-1α and its downstream effector UCP1 was significant in cGK-Tg mice, associated with higher body temperature; however, these changes were not so prominent in BNP-Tg mice. We observed that the functional receptors for NP, GCA, and GCB were abundantly expressed in the brown adipose tissue; however, the clearance receptor (C-receptor) was also rich in the tissue. Therefore, the functional receptor–to–C-receptor ratio, which is suggested to correlate with the biological action of NPs, was lower in the brown adipose tissue than skeletal muscle. We speculate that the abundant expression of C-receptor and the lower ratio of the functional receptors reduced the effect of NP in the brown adipose tissue.

High-fat–fed GCA heterozygous knockout mice accumulated more fat mass and were glucose intolerant compared with wild-type mice. This phenotype is the opposite to that of BNP-Tg or cGK-Tg mice so that the effects of NPs in terms of the prevention of diet-induced obesity and insulin resistance seemed to be mediated at least in part by GCA. We were unable to determine whether GCB also participated because GCB knockout mice were not available. The NP receptors were regulated by dietary conditions; that is, GCA and GCB were upregulated by fasting and downregulated during high-fat feeding. On the other hand, the C-receptor showed opposite kinetics. Therefore, the ratio of functional receptors to C-receptor was lowered by feeding or during chronic high-fat diet; conversely, fasting increased relative amount of the functional receptors. These results indicate that a high-fat diet can contribute to the development of diet-induced obesity and insulin resistance at least partly by downregulation of GCA and upregulation of the C-receptor. The notion that the kinetics of NP receptor expression depend on dietary conditions, such as high-fat diet or fasting, is consistent with earlier findings of others. The GCA–to–C-receptor ratio was shown to be lowered in obese people than in nonobese (28). Natriuresis is known to be increased after several hours of fasting, despite the fact that sodium intake is decreased (29). The upregulation of functional NP receptors in renal tubular cells by fasting and subsequent augmentation of natriuresis might account for the

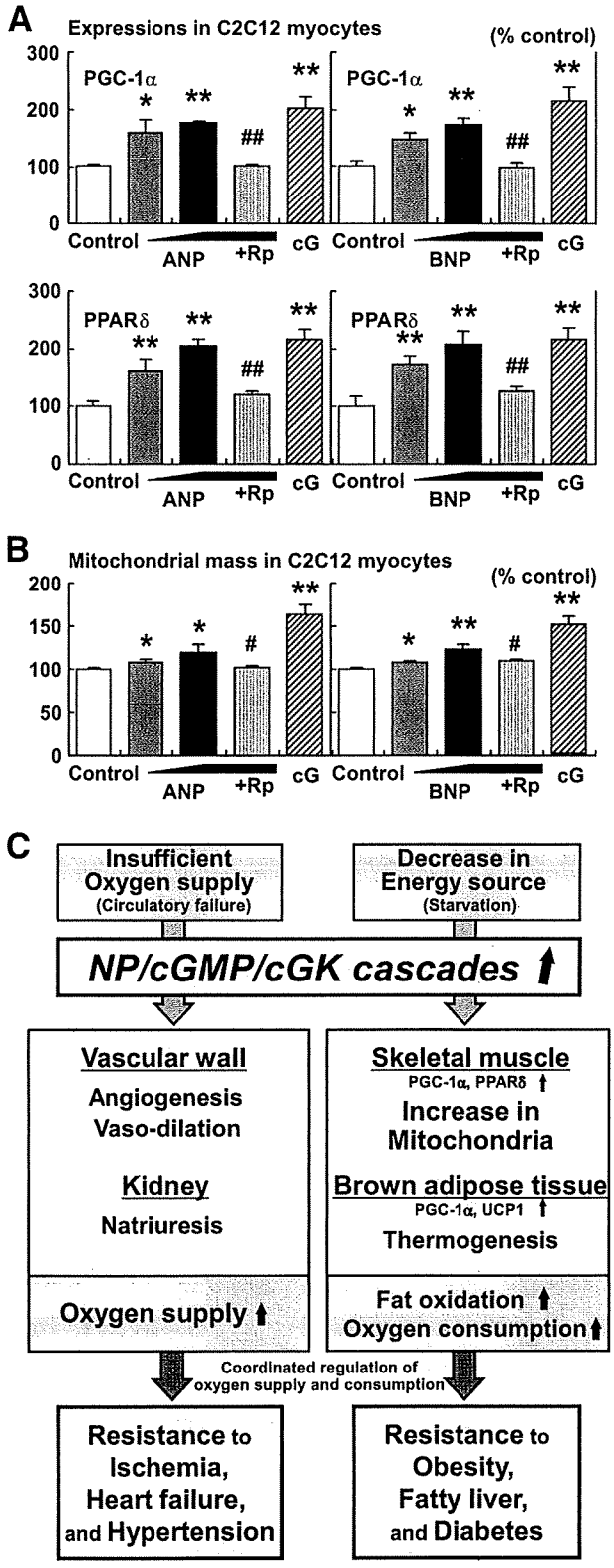

FIG. 6. NPs directly increase the expression of PGC-1α and PPARδ and mitochondrial content in cultured myocytes. C2C12 myocytes were stimulated with the indicated agents for 8 (*A*) or 48 (*B*) hours (ANP 10^{-11}–$^{-9}$ mol/l or BNP 10^{-11}–$^{-9}$ mol/l, with or without the cGMP antagonist, Rp-8-br-cGMP [Rp] 10^{-4} mol/l). Stimulation of cGK by 8-Br-cGMP (cG) 10^{-4} mol/l was also challenged (n = 12). *A*: Gene expressions of PGC-1α and PPARδ in C2C12 cells when treated with ANPs or BNPs. *B*: Mitochondrial mass in C2C12 cells quantified by use of MitoTracker Green, a fluorescent probe for mitochondria. *P < 0.05; **P < 0.01 vs. control; #P < 0.05; ##P < 0.01 vs. the NP (10^{-9} mol/l)-treated group. Rp, Rp-8-br-cGMP (cGMP antagonist), cG, 8-Br-cGMP (membrane-permeable cGMP analog). *C*: Schematic representation of the suggested roles for NP/cGK cascades. Previous studies have shown the significant roles for NP/cGK cascades in the cardiovascular system that lead to resistance to ischemia, heart failure, and hypertension. In the present study, NP/cGK cascades are suggested to promote muscle mitochondrial biogenesis and fat oxidation, as to prevent obesity, fatty liver, and glucose intolerance.

well-known phenomenon of "fasting-induced natriuresis." Taken together, the dietary regulation of the receptor expressions indicates that the signal transduction through NP/cGK cascades, which is augmented by starvation, might have a role in fasting-induced fat oxidation under physiological conditions.

Augmented production of NPs caused by congestive heart failure plays important roles in compensating for the volume expansion and subsequent decrease in oxygen supply by exerting vasodilating, natriuretic, and neurohumoral-modulating actions (30). This compensatory effect in the cardiovascular system has been thought to be the primary role for NP/cGK cascades (31). In the present study, we reveal the new roles for the cascades on mitochondrial biogenesis and fat oxidation through upregulation of PGC-1α and PPARδ. The results of the present study are in line with earlier publications from Lafontan and colleagues (6,7,32,33), which have demonstrated the importance of the NP/cGK system in the regulation of adipose tissue lipolysis. Their results and ours together support the view that NP/cGK cascades have significant roles in lipid catabolism. Moreover, the increase in circulating NP and cGMP levels during exercise has been demonstrated in previous reports (24,25). Therefore, NP/cGMP/cGK cascades might have significant roles in metabolic adaptations in response to exercise, including mitochondrial biogenesis and fat oxidation.

Several other vascular hormones that regulate vascular tone, including catecholamines, angiotensin II, and NO, are also implicated in the regulation of cellular metabolism and subsequent change in body weight and glucose tolerance (34–38). In this context, vascular hormones seem to lie at the crossroad of cardiovascular and metabolic diseases. In a recent report (9), the number of risk factors acting as diagnostic markers of metabolic syndrome is shown to inversely correlate with plasma concentrations of NPs. The clinical data and the findings of the present study collectively indicate that insufficient activation of NP/cGK cascades can be a causative factor of both obesity and hypertension. We speculate that the state of overnutrition would downregulate functional NP receptors as to promote both obesity and hypertension. Furthermore, we believe that physiological responses of vascular hormones, in accordance with blood pressure, circulating fluid volume, and oxygen demand, would result in coordinated regulation of oxygen supply and consumption, and the coordination is especially important for the adaptive responses to exercise.

To summarize, the results of the present study indicate that NP/cGK cascades can promote muscle mitochondrial biogenesis and fat oxidation through upregulation of PGC-1α and PPARδ, as to prevent obesity and glucose intolerance. The results were compatible with our recent report (10), which showed that cGMP can increase mitochondrial content and function in cultured myocytes. The pharmaceutical interventions that activate NP/cGMP/cGK

cascades seem to be potentially beneficial for the treatment of obesity, fatty liver, and glucose intolerance.

ACKNOWLEDGMENTS

This work was supported by grants from Japanese Ministry of Education, Culture, Sports, Science, and Technology; the Ministry of Health, Labor, and Welfare; the University of Kyoto 21st Century Centers of Excellence Program; and grants from the Takeda Medical Research Foundation and the Smoking Research Foundation. The funders had no role in study design, data collection and analysis, decision to publish, or preparation of the manuscript.

No potential conflicts of interest relevant to this article were reported.

K.M. designed the experiments, maintained the mice, performed the experiments, analyzed the data, and wrote the article. H.I. directed the study, contributed to discussion, and edited the manuscript. H.T. supported the study with superb technical assistances and contributed to discussion. N.T., Y.F., M.S., K.Y., D.T., M.I., and T.S. contributed to discussion. K.N. contributed to discussion and encouraged the authors.

We thank T. Shibakusa, K. Inoue, and T. Fushiki in Kyoto University Graduate School of Agriculture and T. Nakamura and H. Sakaue in Kobe University Graduate School of Medicine for technical assistance.

GenBank accession numbers were PGC-1α, NM_008904; PPARδ, NM_011145; UCP1, NM_009463; ATPsyn, NM_007505; COX, NM_009941; UCP3, NM_009464; FATP, NM_011977; ACO, NM_015729; and CPT1b, NM_009948.

REFERENCES

1. Potter LR, Abbey-Hosch S, Dickey DM. Natriuretic peptides, their receptors, and cyclic guanosine monophosphate-dependent signaling functions. Endocr Rev 2006;27:47–72
2. Colucci WS, Elkayam U, Horton DP, Abraham WT, Bourge RC, Johnson AD, Wagoner LE, Givertz MM, Liang CS, Neibaur M, Haught WH, LeJemtel TH. Intravenous nesiritide, a natriuretic peptide, in the treatment of decompensated congestive heart failure. Nesiritide Study Group. N Engl J Med 2000;343:246–253
3. Yamahara K, Itoh H, Chun TH, Ogawa Y, Yamashita J, Sawada N, Fukunaga Y, Sone M, Yurugi-Kobayashi T, Miyashita K, Tsujimoto H, Kook H, Feil R, Garbers DL, Hofmann F, Nakao K. Significance and therapeutic potential of the natriuretic peptides/cGMP/cGMP-dependent protein kinase pathway in vascular regeneration. Proc Natl Acad Sci USA 2003;100:3404–3409
4. Park K, Itoh H, Yamahara K, Sone M, Miyashita K, Oyamada N, Sawada N, Taura D, Inuzuka M, Sonoyama T, Tsujimoto H, Fukunaga Y, Tamura N, Nakao K. Therapeutic potential of atrial nariuretic peptide administration on peripheral arterial diseases. Endocrinology 2008;149:483–491
5. Yasoda A, Komatsu Y, Chusho H, Miyazawa T, Ozasa A, Miura M, Kurihara T, Rogi T, Tanaka S, Suda M, Tamura N, Ogawa Y, Nakao K. Overexpression of CNP in chondrocytes rescues achondroplasia through a MAPK-dependent pathway. Nat Med 2004;10:80–86
6. Sengenes C, Berlan M, De Glisezinski I, Lafontan M, Galitzky J. Natriuretic peptides: a new lipolytic pathway in human adipocytes. FASEB J 2000;14:1345–1351
7. Sengenes C, Bouloumie A, Hauner H, Berlan M, Busse R, Lafontan M, Galitzky J. Involvement of a cGMP-dependent pathway in the natriuretic peptide-mediated hormone-sensitive lipase phosphorylation in human adipocytes. J Biol Chem 2003;278:48617–48626
8. Wang TJ, Larson MG, Levy D, Benjamin EJ, Leip EP, Wilson PW, Vasan RS. Impact of obesity on plasma natriuretic peptide levels. Circulation 2004;109:594–600
9. Wang TJ, Larson MG, Keyes MJ, Levy D, Benjamin EJ, Vasan RS. Association of plasma natriuretic peptide levels with metabolic risk factors in ambulatory individuals. Circulation 2007;115:1345–1353
10. Mitsuishi M, Miyashita K, Itoh H. cGMP rescues mitochondrial dysfunction induced by glucose and insulin in myocytes. Biochem Biophys Res Commun 2008;367:840–845
11. Ogawa Y, Itoh H, Tamura N, Suga S, Yoshimasa T, Uehira M, Matsuda S, Shiono S, Nishimoto H, Nakao K. Molecular cloning of the complementary DNA and gene that encode mouse brain natriuretic peptide and generation of transgenic mice that overexpress the brain natriuretic peptide gene. J Clin Invest 1994;93:1911–1921
12. Lopez MJ, Wong SK, Kishimoto I, Dubois S, Mach V, Friesen J, Garbers DL, Beuve A. Salt-resistant hypertension in mice lacking the guanylyl cyclase-A receptor for atrial natriuretic peptide. Nature 1995;378:65–68
13. Sakai T, Sakaue H, Nakamura T, Okada M, Matsuki Y, Watanabe E, Hiramatsu R, Nakayama K, Nakayama KI, Kasuga M. Skp2 controls adipocyte proliferation during the development of obesity. J Biol Chem 2007;282:2038–2046
14. Shibakusa T, Mizunoya W, Okabe Y, Matsumura S, Iwaki Y, Okuno A, Shibata K, Inoue K, Fushiki T. Transforming growth factor-beta in the brain is activated by exercise and increases mobilization of fat-related energy substrates in rats. Am J Physiol Regul Integr Comp Physiol 2007;292:R1851–R1861
15. Jequier E, Acheson K, Schutz Y. Assessment of energy expenditure and fuel utilization in man. Annu Rev Nutr 1987;7:187–208
16. Lagouge M, Argmann C, Gerhart-Hines Z, Meziane H, Lerin C, Daussin F, Messadeq N, Milne J, Lambert P, Elliott P, Geny B, Laakso M, Puigserver P, Auwerx J. Resveratrol improves mitochondrial function and protects against metabolic disease by activating SIRT1 and PGC-1alpha. Cell 2006;127:1109–1122
17. Itoh H, Nakao K, Mukoyama M, Yamada T, Hosoda K, Shirakami G, Morii N, Sugawara A, Saito Y, Shiono S, Arai H, Yoshida I, Imura H. Chronic blockade of endogenous atrial natriuretic polypeptide (ANP) by monoclonal antibody against ANP accelerates the development of hypertension in spontaneously hypertensive and deoxycorticosterone acetate-salt-hypertensive rats. J Clin Invest 1989;84:145–154
18. Lin J, Handschin C, Spiegelman BM. Metabolic control through the PGC-1 family of transcription coactivators. Cell Metab 2005;1:361–370
19. Barish GD, Narkar VA, Evans RM. PPAR delta: a dagger in the heart of the metabolic syndrome. J Clin Invest 2006;116:590–597
20. Wang YX, Zhang CL, Yu RT, Cho HK, Nelson MC, Bayuga-Ocampo CR, Ham J, Kang H, Evans RM. Regulation of muscle fiber type and running endurance by PPARdelta. PLoS Biol 2004;2:e294
21. Tanaka T, Yamamoto J, Iwasaki S, Asaba H, Hamura H, Ikeda Y, Watanabe M, Magoori K, Ioka RX, Tachibana K, Watanabe Y, Uchiyama Y, Sumi K, Iguchi H, Ito S, Doi T, Hamakubo T, Naito M, Auwerx J, Yanagisawa M, Kodama T, Sakai J. Activation of peroxisome proliferator-activated receptor delta induces fatty acid beta-oxidation in skeletal muscle and attenuates metabolic syndrome. Proc Natl Acad Sci USA 2003;100:15924–15929
22. Luquet S, Lopez-Soriano J, Holst D, Fredenrich A, Melki J, Rassoulzadegan M, Grimaldi PA. Peroxisome proliferator-activated receptor delta controls muscle development and oxidative capability. FASEB J 2003;17:2299–2301
23. Choi CS, Befroy DE, Codella R, Kim S, Reznick RM, Hwang YJ, Liu ZX, Lee HY, Distefano A, Samuel VT, Zhang D, Cline GW, Handschin C, Lin J, Petersen KF, Spiegelman BM, Shulman GI. Paradoxical effects of increased expression of PGC-1alpha on muscle mitochondrial function and insulin-stimulated muscle glucose metabolism. Proc Natl Acad Sci USA 2008;105:19926–19931
24. Moro C, Crampes F, Sengenes C, De Glisezinski I, Galitzky J, Thalamas C, Lafontan M, Berlan M. Atrial natriuretic peptide contributes to physiological control of lipid mobilization in humans. FASEB J 2004;18:908–910
25. Ruskoaho H, Kinnunen P, Taskinen T, Vuolteenaho O, Leppäluoto J, Takala TE. Regulation of ventricular atrial natriuretic peptide release in hypertrophied rat myocardium: effects of exercise. Circulation 1989;80:390–400
26. Arita Y, Kihara S, Ouchi N, Takahashi M, Maeda K, Miyagawa J, Hotta K, Shimomura I, Nakamura T, Miyaoka K, Kuriyama H, Nishida M, Yamashita S, Okubo K, Matsubara K, Muraguchi M, Ohmoto Y, Funahashi T, Matsuzawa Y. Paradoxical decrease of an adipose-specific protein, adiponectin, in obesity. Biochem Biophys Res Commun 1999;257:79–83
27. Yamauchi T, Kamon J, Waki H, Terauchi Y, Kubota N, Hara K, Mori Y, Ide T, Murakami K, Tsuboyama-Kasaoka N, Ezaki O, Akanuma Y, Gavrilova O, Vinson C, Reitman ML, Kagechika H, Shudo K, Yoda M, Nakano Y, Tobe K, Nagai R, Kimura S, Tomita M, Froguel P, Kadowaki T. The fat-derived hormone adiponectin reverses insulin resistance associated with both lipoatrophy and obesity. Nat Med 2001;7:941–946
28. Dessì-Fulgheri P, Sarzani R, Rappelli A. The natriuretic peptide system in obesity-related hypertension: new pathophysiological aspects. J Nephrol 1998;11:296–299
29. Szénási G, Bencsáth P, Szalay L, Takács L. Fasting induces denervation natriuresis in the conscious rat. Am J Physiol 1985;249:F753–F758

30. Mukoyama M, Nakao K, Saito Y, Ogawa Y, Hosoda K, Suga S, Shirakami G, Jougasaki M, Imura H. Increased human brain natriuretic peptide in congestive heart failure. N Engl J Med 1990;323:757–758
31. Boerrigter G, Burnett JC Jr. Recent advances in natriuretic peptides in congestive heart failure. 2004. Expert Opin Investig Drugs. 13: 643–652
32. Moro C, Polak J, Hejnova J, Klimcakova E, Crampes F, Stich V, Lafontan M, Berlan M. Atrial natriuretic peptide stimulates lipid mobilization during repeated bouts of endurance exercise. Am J Physiol Endocrinol Metab 2006;290:E864–E869
33. Lafontan M, Moro C, Berlan M, Crampes F, Sengenes C, Galitzky J. Control of lipolysis by natriuretic peptides and cyclic GMP. Trends Endocrinol Metab 2008;19:130–137
34. Mitsuishi M, Miyashita K, Muraki A, Itoh H. Angiotensin II reduces mitochondrial content in skeletal muscle and affects glycemic control. Diabetes 2009;58:710–717
35. Massiera F, Seydoux J, Geloen A, Quignard-Boulange A, Turban S, Saint-Marc P, Fukamizu A, Negrel R, Ailhaud G, Teboul M. Angiotensinogen-deficient mice exhibit impairment of diet-induced weight gain with alteration in adipose tissue development and increased locomotor activity. Endocrinology 2001;142:5220–5225
36. Bachman ES, Dhillon H, Zhang CY, Cinti S, Bianco AC, Kobilka BK, Lowell BB. betaAR signaling required for diet-induced thermogenesis and obesity resistance. Science 2002;297:843–845
37. Duplain H, Burcelin R, Sartori C, Cook S, Egli M, Lepori M, Vollenweider P, Pedrazzini T, Nicod P, Thorens B, Scherrer U. Insulin resistance, hyperlipidemia, and hypertension in mice lacking endothelial nitric oxide synthase. Circulation 2001;104:342–345
38. Shankar RR, Wu Y, Shen HQ, Zhu JS, Baron AD. Mice with gene disruption of both endothelial and neuronal nitric oxide synthase exhibit insulin resistance. Diabetes 2000;49:684–687

Induction and Isolation of Vascular Cells From Human Induced Pluripotent Stem Cells—Brief Report

Daisuke Taura, Masakatsu Sone, Koichiro Homma, Naofumi Oyamada, Kazutoshi Takahashi, Naohisa Tamura, Shinya Yamanaka, Kazuwa Nakao

Objective—Induced pluripotent stem (iPS) cells are a novel stem cell population derived from human adult somatic cells through reprogramming using a defined set of transcription factors. Our aim was to determine the features of the directed differentiation of human iPS cells into vascular endothelial cells (ECs) and mural cells (MCs), and to compare that process with human embryonic stem (hES) cells.

Methods and Results—We previously established a system for differentiating hES cells into vascular cells. We applied this system to human iPS cells and examined their directed differentiation. After differentiation, TRA1–60$^-$ Flk1$^+$ cells emerged and divided into VE-cadherin–positive and –negative populations. The former were also positive for CD34, CD31, and eNOS and were consistent with ECs. The latter differentiated into MCs, which expressed smooth muscle α-actin and calponin after further differentiation. The efficiency of the differentiation was comparable to that of human ES cells.

Conclusions—We succeeded in inducing and isolating human vascular cells from iPS cells and indicate that the properties of human iPS cell differentiation into vascular cells are nearly identical to those of hES cells. This work will contribute to our understanding of human vascular differentiation/development and to the development of vascular regenerative medicine. (*Arterioscler Thromb Vasc Biol.* **2009;29:1100-1103.**)

Key Words: angiogenesis ■ stem cells ■ vascular biology ■ endothelium ■ differentiation

Pluripotent embryonic stem (ES) cells are thought to represent a potentially unlimited pool from which to derive cells for new treatments in the area of regenerative medicine and for investigation of cell development/differentiation. We previously described the process by which mouse, monkey and human embryonic stem (ES) cells differentiate into vascular cells.[1,2,3] In addition, we used the hindlimb ischemia model with immunodeficient mice to demonstrate that transplanted vascular endothelial cells (ECs) and mural cells (MCs) derived from human (h)ES cells could be successfully incorporated into the host vasculature and significantly accelerate improvements in local blood flow.[3,4] However, immunologic and ethical problems remain to be overcome before clinical application.

Recently, novel ES cell-like pluripotent cells were generated from mouse skin fibroblasts by introducing 4 transcription factors.[5] Termed induced pluripotent stem (iPS) cells, they were subsequently generated from human skin fibroblasts.[6,7] At present, the properties of human iPS cell differentiation into vascular cells remain unknown. To address that issue, we investigated the differentiation of human iPS cells into ECs and MCs using our differentiation system previously developed for hES cells.

Materials and Methods

Cell Culture

hES, human iPS, and OP9 feeder cells were all established and maintained as described previously.[6,8,9] To induce differentiation, hES or iPS cells were cultured on an OP9 feeder layer as described previously.[3]

Flow Cytometry and Cell Sorting

Flow cytometric analysis and cell sorting were performed as described previously.[1,9]

Immunohistochemistry

Cultured cells were stained with various monoclonal antibodies as described.[1,9]

For details regarding cell culture, RT-PCR, and the antibodies used in flow cytometry and immunohistochemistry, please see the supplemental material (available online at http://atvb.ahajournals.org).

Received December 4, 2008; revision accepted April 16, 2009.

From the Department of Medicine and Clinical Science (D.T., M.S., K.H., N.O., N.T., K.N.), Kyoto University Graduate School of Medicine; the Department of Stem Cell Biology (K.T., S.Y.), Institute for Frontier Medical Sciences, Kyoto University; and the Center for iPS Cell Research and Application (CiRA) (K.T., S.Y.), Institute for Integrated Cell-Material Sciences, Kyoto University, Japan.

Correspondence to Masakatsu Sone, MD, PhD, 54 Shogoin Kawahara-cho, Sakyo-ku, Kyoto 606-8507, Japan. E-mail sonemasa@kuhp.kyoto-u.ac.jp

Arterioscler Thromb Vasc Biol **is available at http://atvb.ahajournals.org** **DOI: 10.1161/ATVBAHA.108.182162**

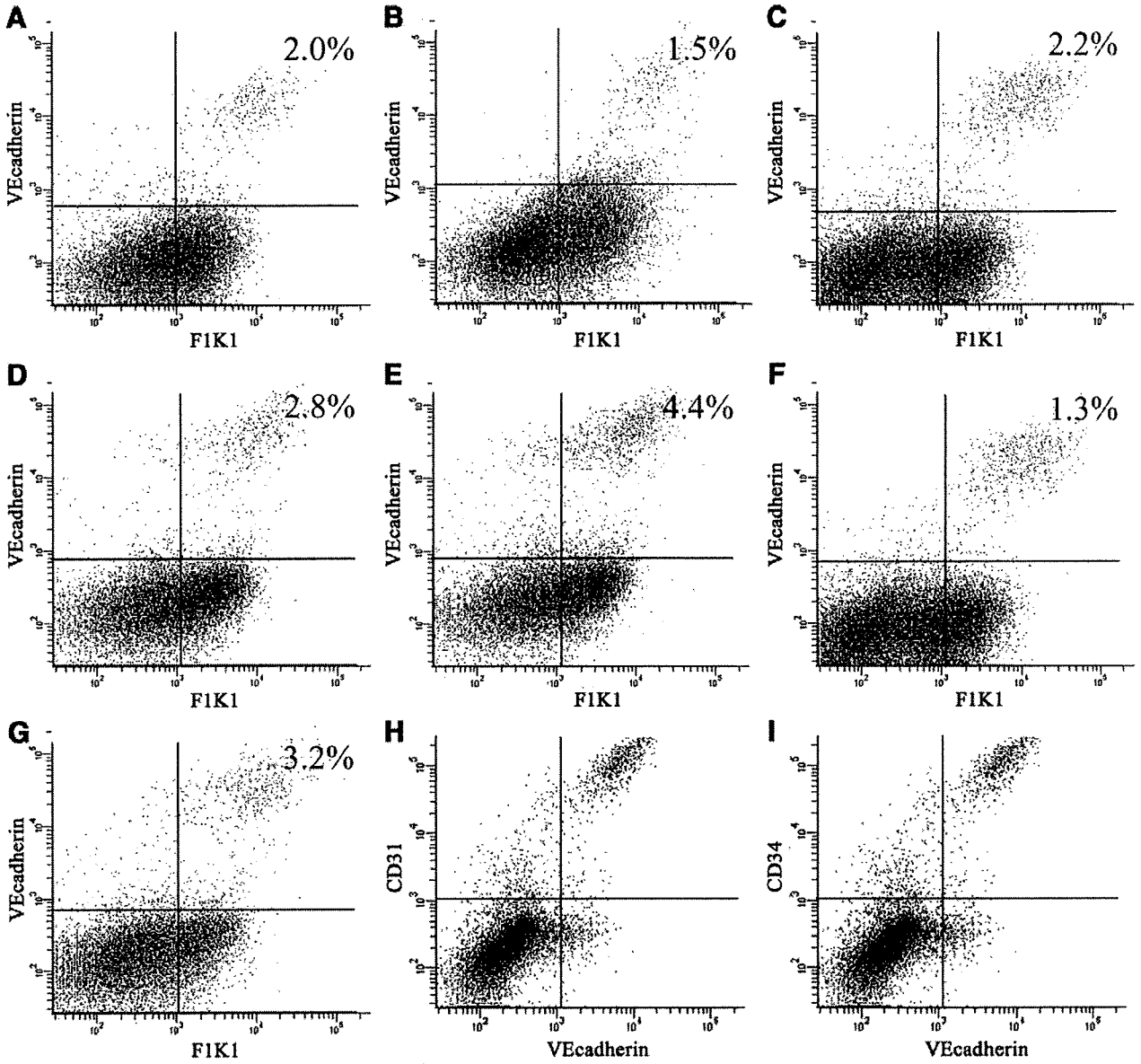

Figure 1. Flow cytometric analysis of hES-derived and iPS-derived cells on day 10 of differentiation. A through C, hES-derived cells (A, H9; B, HES3; C, KhES-1). D through G, iPS-derived cells (D, B6; E, B7; F, G1; G, G4). H and I, Analysis of human iPS-derived cells with other EC markers.

Results

We investigated 3 hES cell lines (H9, HES3, and KhES1) and 4 iPS cell lines (201B6, 201B7, 253G1, and 253G4).[5,6] 201B6 (B6) and 201B7 (B7) cells were generated from human skin fibroblasts by transfection with 4 transcription factors (Oct3/4, Sox2, Klf4, c-Myc), whereas 253G1 (G1) and 253G4 (G4) were generated using only 3 factors (c-Myc was omitted).[10] The morphology of these 4 lines did not differ from hES cells, and they were also positive for hES cell markers (supplemental Figure I). We induced differentiation of these iPS cell lines in an in vitro 2D culture system previously established for differentiation of hES cells into vascular cells.[3] After 10 days of differentiation, cells positive for Flk1 (also designated VEGF receptor-2) and the EC marker VE-cadherin emerged and accounted for 1% to 5% of the cells (Figure 1A through 1G). We noted no differences in the differentiation of the B and G lines, and both were comparable to the hES lines (Figure 1A through 1G). The $Flk1^+$ VE-$cadherin^+$ cell population was also positive for CD31 and CD34 (Figure 1H and 1I), and negative for the ES cell marker tumor rejection antigen 1–60 (TRA1–60). We sorted those cells and recultured with VEGF, and found that they formed a network-like structure on Matrigel, in vitro (Figure 2A), and had a cobblestone appearance when confluent on collagen IV-coated dishes (Figure 2B). Immunofluorescent staining for CD31 produced a characteristic marginal staining pattern (Figure 2C), and staining for endothelial NO synthase produced a cytoplasmic pattern (Figure 2D). Based on these observations, the cells were consistent with ECs. Subsequent RT-PCR analysis of EC markers revealed that both human iPS-derived and hES-derived ECs expressed

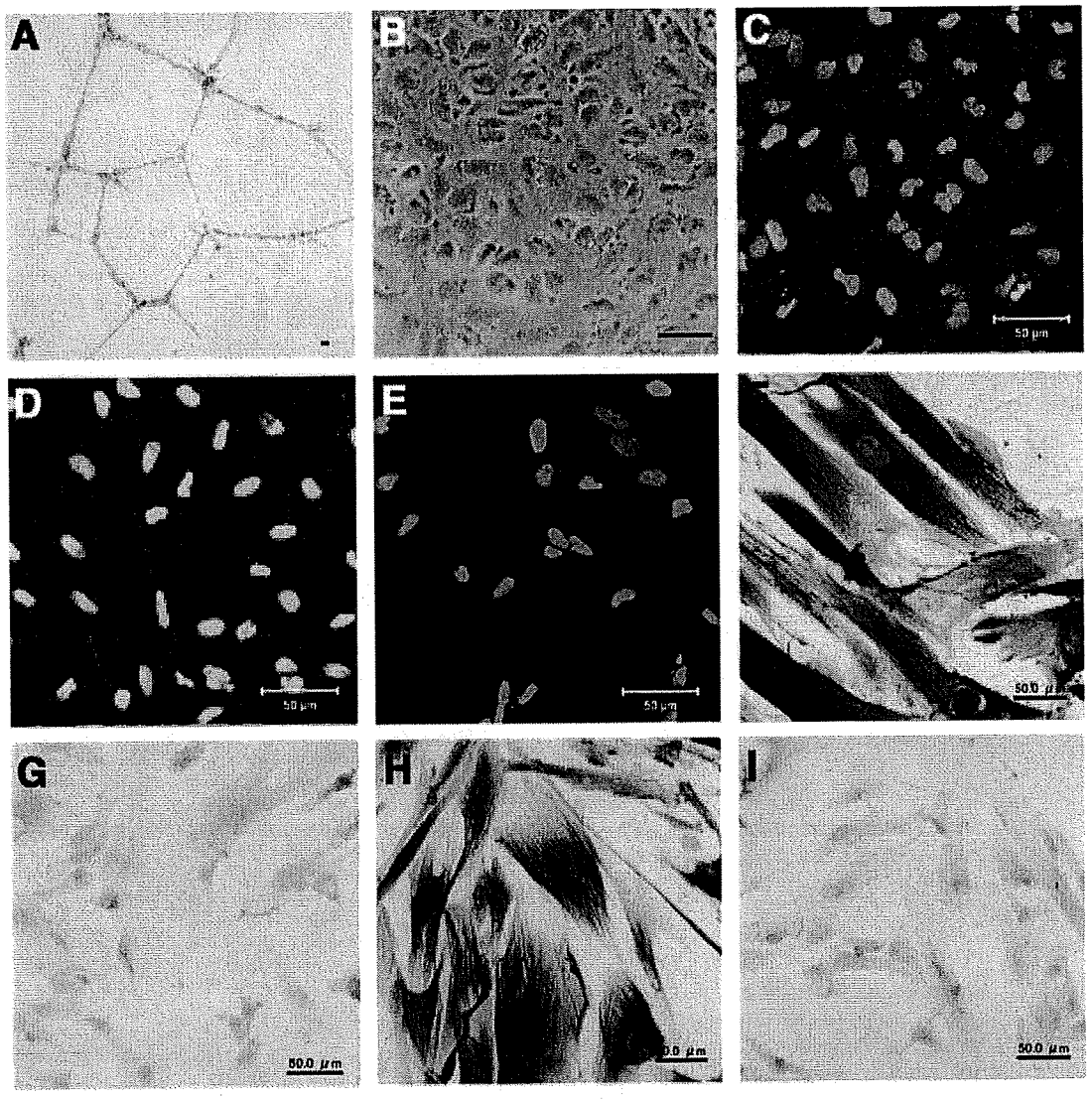

Figure 2. A, Network formation by iPS-derived VE-cadherin$^+$ cells after 24 hours of culture on Matrigel. B, Phase-contrast photomicrograph of iPS-derived VE-cadherin$^+$ cells. C through E, Immunostaining of VE-cadherin$^+$ cells: red, CD31 (C) or eNOS (D) or control mouse IgG1 (E; as negative control for C and D); green, nuclei. F through I, Immunostaining of VE-cadherin$^-$ Flk1$^+$ cells for MC markers: F, αSMA; G, control mouse IgG2 (negative control for F); H, calponin; I, control mouse IgG1 κ (negative control for H). Scale bars=50 μm.

VE-cadherin, CD31, von Willebrand factor (vWF), and CD34 at levels similar to those seen in adult ECs (supplemental Figure II).

We next sorted for Flk1$^+$ VE-cadherin$^-$ TRA1–60$^-$ cells on day 10 of differentiation and then induced differentiation into MCs using PDGF-BB as described previously.[3,4] Once differentiated, these cells stained positively for αSMA and calponin and were therefore consistent with MCs (Figure 2E and 2F). Both human iPS-derived and hES-derived MCs expressed the vascular smooth cell markers at levels similar to those seen in adult vascular smooth muscle cells (supplemental Figure II).

Discussion

The establishment of iPS cells opened a new avenue for regenerative medicine and stem cell biology. The directional differentiation of mouse iPS cells into vascular cells was recently reported.[11] In the present study, we have shown that human iPS cells can be directionally differentiated into vascular ECs and MCs by applying the same methods we established for hES cells.[3] We previously reported that the differentiation kinetics of primate ES cells to vascular cells is not equal to that of mouse ES cells.[2,3] To further clarify the differentiation process in human beings and to determine the possible clinical application of iPS cells, investigation of human iPS cells is essential because some characters were significantly different between mouse and human iPS cells as ES cells.

In contrast to human ES cells, iPS cells can be established from every human being irrespective of their genetic backgrounds. The establishment of in vitro differentiation system of human vascular cells from human iPS cells should make it possible to dissect out cellular mechanisms

in human vascular development and diseased states such as arteriosclerosis. The establishment of iPS cell lines from patients with inherited diseases presenting vascular abnormality should enable clarification of their pathogenesis. In addition, because they overcome the immunologic and ethical problems associated with human ES cells, our study should also contribute to the development of novel patient-specific cell based vascular regenerative therapies.

Several issues remain to be resolved before human iPS-derived vascular cells can be administered to humans, however. Although we observed no reappearance of undifferentiated or tumor cell-like structures in the in vitro cultures, when we examined the mRNA expression of the transgenes during differentiation experiments, we occasionally observed upregulation of the transgenic mRNA (supplemental Figure III). The safety of iPS cells needs to be confirmed for each iPS cell line, both in vitro and in vivo.

In conclusion, we succeeded in inducing and isolating human vascular cells from iPS cells and indicate that the properties of differentiation are nearly identical to those of hES cells. This work will contribute to our understanding of human vascular differentiation/development and to the development of vascular regenerative medicine.

We described additional discussions about the safety of iPS cells in the supplemental material.

Acknowledgments

We thank Yoshie Fukuchi for her technical assistance. The antihuman Flk1 antibody (KM1668) was a generous gift from Kyowa Hakko Co Ltd.

Sources of Funding

This work was supported by the project for realization of regenerative medicine of the Ministry of Education, Culture, Sports, Science, and Technology, Japan, Grants-in-Aid for Scientific Research from the Ministry of Health, Labor, and Welfare, the Ministry of Education, Culture, Sports, Science, and Technology, the Takeda Science Foundation, the Japan Cardiovascular Research Foundation, and the Smoking Research Foundation.

Disclosures

None.

References

1. Yamashita J, Itoh H, Hirashima M, Ogawa M, Nishikawa S, Yurugi T, Naito M, Nakao K, Nishikawa S. Flk1-positive cells derived from embryonic stem cells serve as vascular progenitors. *Nature*. 2000;408:92–96.
2. Sone M, Itoh H, Yamashita J, Yurugi-Kobayashi T, Suzuki Y, Kondo Y, Nonoguchi A, Sawada N, Yamahara K, Miyashita K, Park K, Shibuya M, Nito S, Nishikawa S, Nakao K. Different differentiation kinetics of vascular progenitor cells in primate and mouse embryonic stem cells. *Circulation*. 2003;107:2085–2088.
3. Sone M, Itoh H, Kenichi Yamahara, Yamashita J, Yurugi-K T, Nonoguchi A, Suzuki Y, Chao TH, Sawada N, Fukunaga Y, Miyashita K, Park K, Oyamada N, Sawada N, Taura D, Tamura N, Kondo Y, Nito S, Suemori H, Nakatsuji N, Nishikawa N, Nakao K, Pathway for differentiation of human embryonic stem cells to vascular cell components and their potential for vascular regeneration. *Arterioscler Thromb Vasc Biol*. 2007;27:2127–2134.
4. Yamahara K, Sone M, Itoh H, Yamashita J, Yurugi-K T, Homma K, Chao TH, Miyashita K, Park K, Oyamada N, Sawada N, Taura D, Fukunaga Y, Tamura N, Nakao K. Augmentation of Neovascularizaition in hindlimb ischemia by combined transplantation of human embryonic stem cells-derived endothelial and mural cells. *PLOS one*. 2008;3:e1666.
5. Takahashi K, Yamanaka S. Induction of pluripotent stem cells from mouse embryonic and adult fibroblast cultures by defined factors. *Cell*. 2006;126:663–676.
6. Takahashi K, Tanabe K, Ohnuki M, Narita M, Ichisaka T, Tomoda K, Yamanaka S. Induction of pluripotent stem cells from adult human fibroblasts by defined factors. *Cell*. 2007;131:861–872.
7. Yu J, Vodyanik MA, Smuga-Otto K, Antosiewicz-Bourget J, Frane JL, Tian S, Nie J, Jonsdottir GA, Ruotti V, Stewart R, Slukvin II, Thomson JA. Induced pluripotent stem cell lines derived from human somatic cells. *Science*. 2007;318:1917–1920.
8. Fujioka T, Yasuchika K, Nakamura Y, Nakatsuji N, Suemori H. A simple and efficient cryopreservation method for primate embryonic stem cells. *Int J Dev Biol*. 2004;48:1149–1154.
9. Hirashima M, Kataoka H, Nishikawa S, Matsuyoshi N, Nishikawa S. Maturation of embryonic stem cells into endothelial cells in an in vitro model of vasculogenesis. *Blood*. 1999;93:1253–1263.
10. Nakagawa M, Koyanagi M, Tanabe K, Takahashi K, Ichisaka T, Aoi T, Okita K, Mochiduki Y, Takizawa N, Yamanaka S. Generation of induced pluripotent stem cells without Myc from mouse and human fibroblasts. *Nat Biotechnol*. 2008;26:101–106.
11. Narazaki G, Uosaki H, Teranishi M, Okita K, Kim B, Matsuoka S, Yamanaka S, Yamashita J. Directed and systematic differentiation of cardiovascular cells from mouse induced pluripotent stem cells. *Circulation*. 2008;118:498–506.

Available online at www.sciencedirect.com
ScienceDirect
Metabolism Clinical and Experimental 58 (2009) 1681–1687
Metabolism
Clinical and Experimental
www.metabolismjournal.com

Clinical characteristics and efficacy of pioglitazone in a Japanese diabetic patient with an unusual type of familial partial lipodystrophy

Masanori Iwanishi[a,*], Ken Ebihara[b], Toru Kusakabe[b], Wen Chen[a], Jun Ito[a], Hiroaki Masuzaki[b], Kiminori Hosoda[b], Kazuwa Nakao[b]

[a]*Diabetes and Endocrine Division, Kusatsu General Hospital 1660 Yabase, Kusatsu, Shiga 525-8585, Japan*
[b]*Department on Medicine and Clinical Science, Kyoto University Graduate School of Medicine, Kyoto 606-8507, Japan*
Received 24 September 2008; accepted 7 April 2009

Abstract

This report describes a 46-year-old Japanese diabetic woman with an unusual type of familial partial lipodystrophy. She has marked loss of subcutaneous fat in her lower limbs and buttocks, with sparing of the face, neck, upper limbs, and trunk. This distribution of fat atrophy appears to be rare in comparison with previous reports. Sequencing of candidate genes *LMNA*, *PPARG*, *AKT2*, caveolin-1, as well as the *PPARG4* promoter gene, which are known to be associated with familial partial lipodystrophy, revealed no genetic abnormalities, suggesting that this case may involve a novel gene. Pioglitazone was markedly effective in glycemic control in this case. Her diabetes remained uncontrolled despite a total daily dose of insulin of 30 U and combined treatment with 10 mg of glibenclamide and 0.6 mg of voglibose. We therefore attempted combined treatment with 30 mg of pioglitazone and 30 U/d insulin injection. The hemoglobin A_{1c} level was reduced from 11.2% to 6.1% after 6 months of treatment and has since remained stable. Her body weight increased from 62.0 to 71.0 kg after 12 months of treatment, suggesting that weight gain may result from synergism between thiazolidinediones and insulin-promoting adipogenesis. Pioglitazone increased the fat mass in the upper limbs and trunk, while inducing less increase in the lower limbs, where fat atrophy exists in this patient. Pioglitazone may thus have improved the glycemic control in this case through adipocyte differentiation from progenitor cells mainly in the upper limbs and trunk.

1. Introduction

Understanding of the pathophysiology in lipodystrophy has recently improved [1-4]. Lipodystrophy is a rare disorder characterized by partial or generalized loss of adipose tissue deposits. It is commonly associated with dyslipidemia, hepatic steatosis, and insulin-resistant diabetes. Familial partial lipodystrophy (FPLD) is named after Dunnigan et al [5], who provided a detailed description of the syndrome. In some cases, the lipodystrophy is confined to the limbs, with sparing of the face and trunk, whereas the trunk is also affected with sparing of the face and vulva in other cases. Many cases of FPLD of European origin have been reported to be of the Dunningan et al type, whereas Asian cases of FPLD have only rarely been reported [2,3]. It is thus unclear whether differences in phenotype or genotype of FPLD exist between cases of European origin and of Asian origin. We present here an instructive case of a Japanese diabetic patient with an unusual type of FPLD, with the results of mutational analysis for the *LMNA*, *PPARG*, *AKT2*, and caveolin-1 gene and *PPARG4* promoter gene. We also describe the effectiveness of pioglitazone on glycemic control and the changes of fat and lean mass as measured by dual-energy x-ray absorptiometry (DEXA) scan during pioglitazone treatment.

2. Subject and methods

2.1. Blood samples

Blood was collected after a 12-hour overnight fast for analysis of glucose, insulin, leptin, and adiponectin.

* Corresponding author. Tel.: +1 075 595 0258; fax: +1 075 595 0258.
E-mail address: yuka-1@mx.biwa.ne.jp (M. Iwanishi).

0026-0495/$ – see front matter © 2009 Published by Elsevier Inc.
doi:10.1016/j.metabol.2009.04.043

2.2. Biochemical analyses

Plasma glucose was measured by the glucose oxidase method, and hemoglobin A_{1c} (HbA_{1c}) was measured by a high-performance liquid chromatography method. Serum insulin level was measured using commercial radioimmunoassay kits (Shionogi, Osaka, Japan). Serum leptin level was determined by radioimmunoassay using commercial kits (Linco Research, St Charles, MO). Serum adiponectin level was determined by radioimmunoassay using commercial kits (Otsuka assay, Osaka, Japan) [6].

2.3. Oral glucose tolerance test

A standard oral glucose tolerance test (OGTT) with 75 g of glucose was performed after a 12-hour overnight fast. Venous blood was collected for determination of glucose and insulin concentrations immediately before glucose administration and at 30-minute intervals thereafter for 120 minutes.

2.4. Magnetic resonance imaging technique

Magnetic resonance imaging (MRI) was performed using a 1.5-T imaging device (Sigma Horizon; General Electric, Milwaukee, WI). The upper and lower limbs were surveyed using contiguous axial, 10-mm slices. Fat was easily identified on MRI because of its short T1 relaxation time and its relatively high signal intensity on images compared with other tissues such as muscle.

2.5. Dual-energy x-ray absorptiometry

Whole-body DEXA scan was performed with a multiple detector fan-beam Hologic (Bedford, MA) QDR-4500W densitometer. Data were obtained from the head, upper extremities, trunk, and lower extremities. Proportions of fat in individual regions as well as the whole body were calculated as percentage of body mass. Data were also obtained for measurement of lean tissue mass and bone mineral density.

2.6. Measurement of fat distribution

Subcutaneous and visceral fat distributions were determined by measuring a −150- to −50-Hounsfield unit area using a modification of the method of computed tomographic (CT) scanning (Light Speed Plus-R, General Electric) by Tokunaga et al at the umbilical level [7]. Computed tomographic images were obtained both at baseline and after 9 months of treatment. The V/S ratio was calculated as visceral adipose tissue area divided by subcutaneous adipose tissue area.

2.7. Sequence analyses

Sequence analyses of *LMNA* and *PPARG* were performed in the patient. The patient gave written informed consent for all genetic analyses, which were approved by the Ethical Committee of Kyoto University Graduate School of Medicine. Genomic DNA was isolated from blood using an InstaGene Whole Blood kit (Bio-Rad, Hercules, CA) according to the manufacturer's protocol. Polymerase chain reaction primers, including exon-specific fragments and splice sites, were designed using genomic DNA sequences of human *LMNA* and *PPARG* obtained from GenBank accession numbers NM-170707, AB005520, and AB005526, respectively, as well as published sequences [8,9]. Polymerase chain reaction products were separated by electrophoresis in a 2% agarose gel, purified, and sequenced directly by the chain termination method with both forward and reverse primers on an ABI PRISM310 Genetic Analyzer (PerkinElmer, PE Applied Biosystems, Foster City, CA). All exons and intron-exon boundaries of *AKT2* were amplified and sequenced using primers as previously described [10]. The exons and intron-exon boundaries of caveolin-1 were amplified and bidirectionally sequenced using primers and conditions as previously described [11]. A previously reported method was used to detect the *PPARG4* promoter mutation [12].

3. Case report

The patient is a 46-year-old woman. When she was 34 years old, a diagnosis of diabetes was made by a family physician on the basis of HbA_{1c} and high postprandial glucose levels. However, she decided not to receive any medications for diabetes. She was introduced to our hospital for treatment in December 1998 because of poor glycemic control at 40 years of age. She had a body mass index (BMI) of 23 (height, 160 cm; body weight, 58.5 kg). She had no history of hypertension or autoimmune disease. She was premenopausal status. There was no evidence of axial acanthosis nigricans. In January 1999, HbA_{1c} was 11.6% and her lipid profile was normal (Table 1). An OGTT was performed in September 1999, when she was receiving 10 mg of glibenclamide and 0.6 mg of voglibose and her HbA_{1c} was 8.2%. As shown in Table 2, the insulin levels during OGTT were relatively high, suggesting mild insulin resistance. When serum leptin and adiponectin were measured before her second pioglitazone treatment, she had a BMI of 25.3. Her serum leptin level was 10.4 ng/

Table 1
Biochemical data for this patient

Metabolic variables	Patient
Plasma glucose (mg/dL)	245
HbA_{1c} (%)	11.6
Plasma insulin (μU/mL)	19.1
Serum triglycerides (mg/dL)	137
Serum cholesterol (mg/dL)	200
Serum HDL cholesterol (mg/dL)	49
Serum leptin (ng/mL)	10.4
Serum adiponectin (μg/mL)	3.5

All samples were obtained after a 12-hour overnight fast. HDL indicates high-density lipoprotein.

Table 2
Plasma glucose and insulin levels before and 30, 60, and 120 minutes after an oral 75-g glucose load

	Time (min)			
	0	30	60	120
Plasma glucose (mg/dL)	245	342	409	401
Plasma insulin (μU/mL)	17.7	31.3	79.7	33.0

mL, whereas her serum adiponectin was 3.5 μg/mL (Table 1). An abdominal ultrasound examination revealed hepatic steatosis (unpresented data). She had first noted her decreased subcutaneous fat over her lower limbs at 12 years of age. As shown in Fig. 1B, she exhibited loss of fat in subcutaneous deposits in the lower limbs and buttocks, with prominent lower limbs musculature and excess fat deposition around the face, neck, and trunk. As shown in Fig. 1A, her mother and 2 sisters had a similar physical appearance; and an autosomal dominant pattern of inheritance was therefore considered. A clinical diagnosis of FPLD was therefore made. Her mother had diet-controlled diabetes diagnosed at 75 years of age and died of cerebral infarction at 80 years old. Her father, son, and daughter each had neither fat atrophy nor diabetes mellitus. Her father died of lung cancer at 64 years of age. As shown in Fig. 2, we began initial combined treatment with pioglitazone and insulin injection for diabetes in March 2000, but discontinued pioglitazone in March 2001 because of weight gain. After approximately 3-year washout of pioglitazone, we noted fat atrophy over her lower limbs and assessed body fat distribution by DEXA, MRI, and CT studies in March 2004. As shown in Fig. 1C, T1-weighed MR images at the level of the gluteal fat revealed the striking loss of gluteal subcutaneous fat. As shown in Fig. 1D, axial MRI at the level of the thigh and calf in the patient revealed nearly complete absence of subcutaneous fat in the thigh and calf. As shown in Fig. 1E, axial T1 MRI at the level of the arm and forearm in the patient revealed the preservation of subcutaneous fat. As shown in Fig. 1F, thoracic and abdominal CT revealed preservation of subcutaneous fat in the abdominal and thoracic regions. Table 3 shows the regional and whole-body adipose tissue distribution and body composition estimated by DEXA scan. Compared with healthy subjects, she had markedly decreased fat in her legs, with prominent accumulation in the trunk. Fat accumulation was preserved in her upper limbs. She appeared to have well-preserved skeletal muscle mass.

The first pioglitazone treatment was performed before the diagnosis of FPLD and was markedly effective in improving glycemic control.

Glibenclamide (2.5 mg) and voglibose 0.6 mg/d were started in December 1998; and although the dose of glibenclamide was increased to 10 mg/d, her HbA_{1c} was 9.5% and remained high. Injection of biphasic human insulin (BHI 30) was added at a dose of 16 U/d, and the dose of insulin was increased to 30 U/d; but HbA_{1c} was still 8.0%, and her blood glucose level remained unsatisfactory. Her body weight gain was about 3 kg, and BMI was increased to 24.4 during combined treatment with glibenclamide and insulin. We stopped the glibenclamide and prescribed metformin 500 mg/d, but HbA_{1c} increased to 11.2%. We therefore discontinued the metformin and initiated combined treatment with pioglitazone (30 mg/d) and insulin in March 2000. Her response to pioglitazone was monitored by HbA_{1c}. Fig. 2 shows HbA_{1c} level during treatment. Decline in HbA_{1c} was observed at 2 months; and the decrease continued to be observed throughout the treatment, with lowest values at 6 months. After 6 months of treatment, HbA_{1c} had decreased from 11.2% to 6.1% and remained thereafter at about 6.0%. After 7 months of treatment, the dose of insulin was decreased to 20 U/d. Fig. 2 also shows change in body weight during treatment. After 12 months, body weight had increased from 62.0 to 71.0 kg. We stopped pioglitazone in March 2001 because of this weight gain.

3.1. Changes in body fat distribution and serum adiponectin during the second pioglitazone treatment

About 3 years had passed since she received the combined treatment with 4 mg glimepiride and 30 U/d insulin injection (BHI 30) instead of pioglitazone. Her blood glucose level remained unsatisfactory. We therefore began administration of a half-dose (15 mg) of pioglitazone in April 2004 to prevent body weight gain. Change in fat and lean mass was monitored during pioglitazone treatment by DEXA scan. We also evaluated changes in subcutaneous and visceral fat area by abdominal CT and adiponectin level during pioglitazone treatment. After 9 months of treatment, HbA_{1c} level was reduced from 8.5% to 6.2% and remained stable thereafter, whereas body weight increased by about 3 kg (Fig. 3). As shown in Table 4, comparison of DEXA scan results showed that fat mass increased by 2.2 kg, whereas lean mass increased by 0.7 kg during pioglitazone treatment. Pioglitazone induced increase in fat mass almost equally in the upper limbs, lower limbs, and trunk, although the increase was slightly less in the lower limbs than in the other 2 regions. Interestingly, the increase in lean mass in the lower limbs was greater than that in the upper limbs and trunk, whereas the increase in lean mass in the upper limbs and trunk was suppressed. We also evaluated the accumulation of subcutaneous and visceral fat by CT scan at the umbilical levels before and after 9 months of pioglitazone treatment. Pioglitazone increased subcutaneous fat from 160.0 to 211.3 cm^2, but resulted in almost no change in visceral fat (103.7 vs 106.2 cm^2). After 9 months of treatment, serum adiponectin had increased from 3.5 to 21.7 μg/mL.

3.2. Sequence analysis

We examined the sequences of the entire coding regions and exon-intron boundary regions of the *LMNA*, *PPARG*,

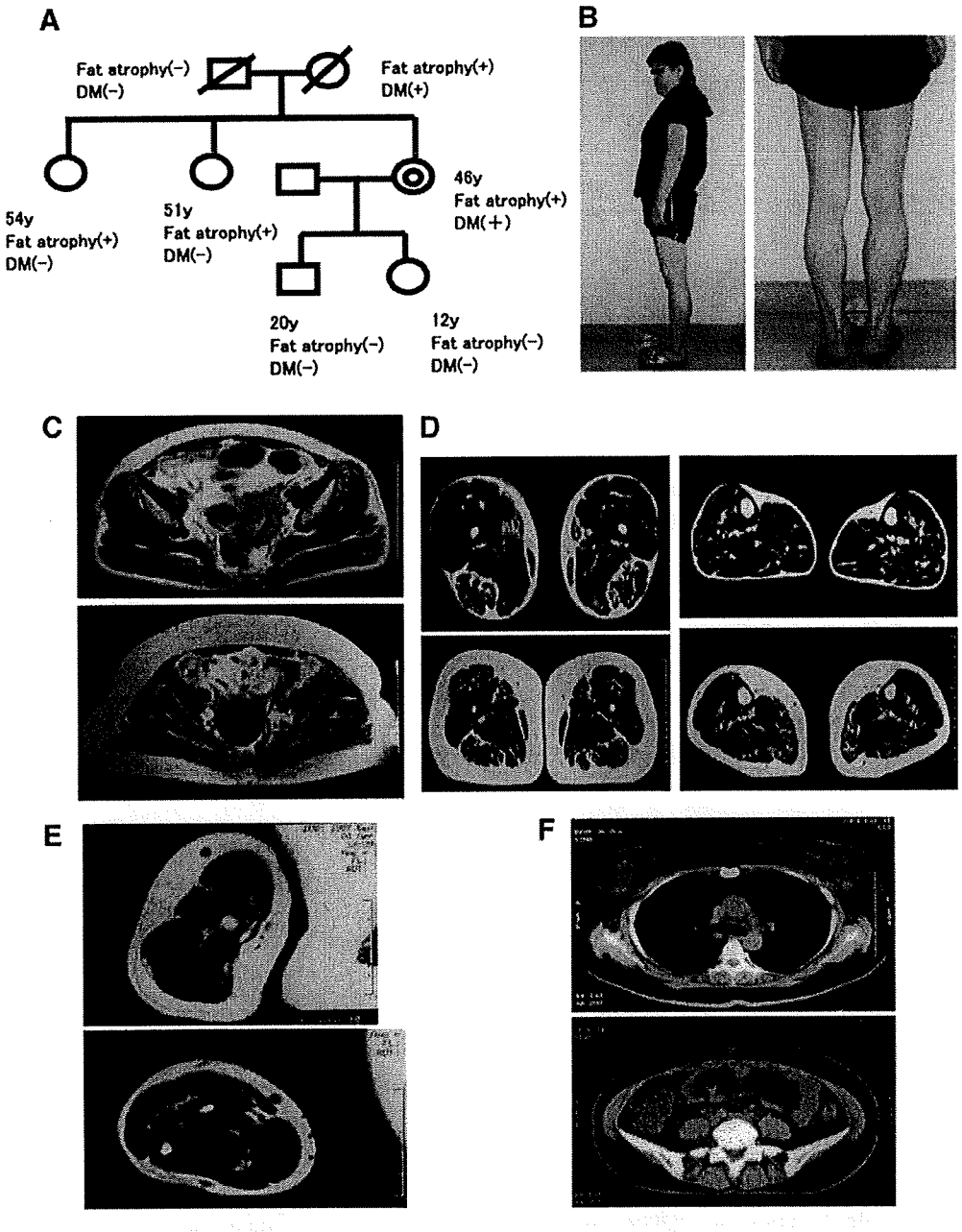

Fig. 1. A, The pedigree of a Japanese family with an unusual type of FPLD. The proband, her mother, and 2 sisters exhibited marked loss of subcutaneous fat in the lower limbs and buttocks. The proband and her mother had diabetes mellitus. B, Phenotypic features of the patient. Note the prominent lower limbs musculature as well as the preservation of abdominal and cervical fat with loss of lower limbs and gluteal fat deposits. C, T1-weighted MR images at the level of the gluteal fat indicate striking loss of gluteal subcutaneous fat in the upper panel. Control images obtained from a healthy female individual are shown in lower panel. D, T1-weighted MR images at the level of the thigh (left panel) and calf (right panel) in the patient reveal nearly complete absence of subcutaneous fat. Control images obtained from a healthy female individual are shown in the lower panel. E, T1-weighted MR images at the level of the arm (upper panel) and forearm (lower panel) in the patient indicate preservation of subcutaneous fat. F, Thoracic CT at the level of the fourth thoracic vertebrae and abdominal CT at the umbilical level. Thoracic (upper panel) and abdominal (lower panel) findings reveal that CT showed the preservation of subcutaneous fat in the abdomen and thoracic region.

AKT2, and caveolin-1 genes, but found no mutations of these genes in the proband. We also checked for −14A>G substitution upstream from exon 1 within the *PPARG4* promoter, but did not find this mutation.

4. Discussion

In this article, we have described a 46-year-old Japanese diabetic woman with an unusual type of FPLD. She has

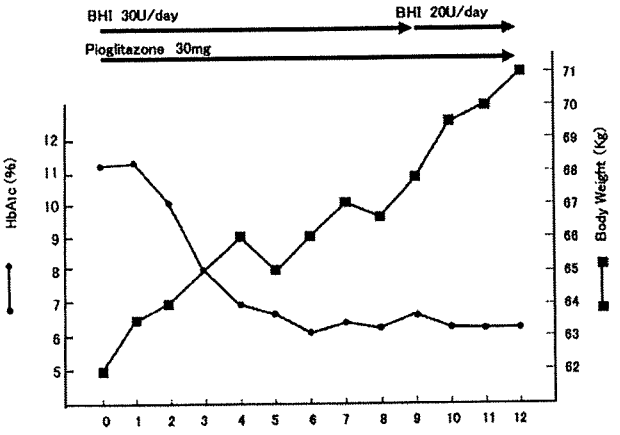

Fig. 2. Hemoglobin A_{1c} level and body weight during the first pioglitazone treatment. Pioglitazone (30 mg) was administered and dramatically improved glycemic control. However, it was stopped because of body weight gain.

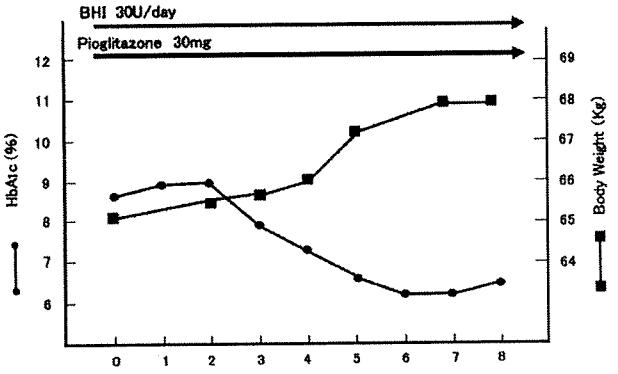

Fig. 3. Hemoglobin A_{1c} level and body weight during the second pioglitazone treatment. The dose of pioglitazone was 15 mg to prevent excessive body weight gain. Changes in body fat composition were evaluated by DEXA scan and abdominal CT as well as serum adiponectin level after 9 months of pioglitazone treatment.

marked loss of subcutaneous fat in her lower limbs and buttocks, with sparing of the face, neck, upper limbs, and trunk. The cases of FPLD reported thus far have predominantly affected the limbs and gluteal fat deposits, with variable truncal involvement but normal or excess fat on the face and neck [2,5,13-16,18-20]. The distribution of fat atrophy in the present case thus appears to be rare.

The loss of body fat in FPLD can be caused by defects in the development and/or differentiation of adipose tissue as a consequence of mutations in a number of genes, including *LMNA*, *PPARG*, *AKT2*, and caveolin-1 [2,15]. Patients with *LMNA* gene mutation have FPLD as indicated by a loss in subcutaneous fat in the upper and lower limbs [2,17]. Patients with *PPARG* gene mutation also have FPLD, as indicated by a loss of fat in subcutaneous deposits in the limbs, affecting the distal regions of the extremities such as the forearms and calves more than the proximal regions, but with preservation of visceral and abdominal subcutaneous fat [2,18-20]. It appears likely that our patient has no mutation of the *LMNA* or *PPARG* gene because she has a phenotype of lipodystrophy distinct from that of patients with *LMNA* gene or *PPARG* gene mutation.

Recently, George et al [10] reported a heterozygous missense mutation R274H in the *AKT2* gene in a family in which affected subjects developed insulin resistance, diabetes mellitus, and hypertension. The proband, a 34-year-old woman, had partial lipodystrophy affecting her extremities. Cao et al [15] also reported a heterozygous

Table 3
Body composition as determined by DEXA scan in the proband

	Proband	Mean values (in control subjects)
Height (cm)	160.0	156.1 ± 4.9
Body weight (kg)	64.0	55.1 ± 6.7
BMI (kg/m^2)	25.0	22.7 ± 3.0
Age (y)	46	45.1 ± 2.8
Fat (%)		
Whole body	33.1	30.3 ± 6.2
1 Arm	42.9	26.9 ± 7.3
1 Leg	13.0	33.2 ± 5.7
Trunk	40.4	28.4 ± 7.7
Fat mass (kg)		
Whole body	20.2	16.8 ± 5.2
1 Arm	1.3	0.7 ± 0.3
1 Leg	0.9	3.5 ± 1.0
Trunk	15.0	7.1 ± 2.8
Lean mass (kg)		
Whole body	38.8	35.3 ± 3.1
1 Arm	1.7	1.7 ± 0.2
1 Leg	5.4	6.6 ± 0.9
Trunk	21.5	16.3 ± 1.3

Normal values are obtained from 55 healthy middle-aged women. Fat, fat mass, and lean mass in 1 arm and leg indicate the mean values of left and right arm (or leg).

Table 4
Changes in fat and lean mass determined by DEXA, subcutaneous and visceral fat areas determined by abdominal CT, and serum adiponectin level during pioglitazone treatment

	Pioglitazone		
	Pre	Post	Change
Body weight (kg)	65.0	68.0	+3.0
Fat (kg)			
Whole body	20.2	22.4	+2.2
Arms	2.7	3.5	+0.8
Legs	1.7	2.2	+0.5
Trunk	15.0	15.9	+0.9
Lean mass (kg)			
Whole body	38.8	39.5	+0.7
Arms	3.3	3.1	−0.2
Legs	10.8	11.9	+1.1
Trunk	21.5	21.3	−0.2
CT (umbilical level)			
Subcutaneous fat (cm^2)	160	211.3	+51.3
Visceral (cm^2)	103.7	106.2	+2.5
Adiponectin (μg/mL)	3.5	21.7	+18.2

caveolin-1 frameshift mutation in patients with atypical partial lipodystrophy and hypertriglyceridemia. We were therefore interested in the possibility of involvement of the *AKT2* and caveolin-1 genes in this case and added mutational analysis, including *AKT2* and caveolin-1. However, we found no mutations in these genes. This case thus features an unusual phenotype, with no mutation of the causing gene in FPLD, *LMNA*, *PPARG*, *AKT2*, caveolin-1, and *PPARG4* promoter. It is thus possible that the present case is due to a defect of a novel gene. However, we could not analyze messenger RNA (mRNA) of candidate gene in this article; and we could not rule out the following possibility. The mutation might be located anywhere except the entire coding regions and exon-intron boundary regions in candidate gene. It might either cause the dysfunction of mRNA of candidate gene or, alternatively, decrease levels of mRNA of candidate gene [21].

Pioglitazone was markedly effective in improving glycemic control in our case. As shown in Fig. 2, HbA_{1c} level decreased by 5.1% in our patient after 6 months of treatment with pioglitazone. Marked weight gain was also observed in our patient during pioglitazone treatment. This observation was compatible with a previous report [14], suggesting that it may result from synergism between thiazolidinediones (TZDs) and insulin-promoting adipogenesis. The level of adiponectin was low before treatment, but increased markedly during pioglitazone treatment. Thiazolidinediones seemed ideally suited to treat lipoatrophic diabetes [22]. Almost all diabetic patients in this study had partial lipodystrophy. In the 13 patients with diabetes who completed 6 months of troglitazone treatment, HbA_{1c} levels significantly decreased by a mean of 2.8%.Troglitazone treatment significantly increased body fat without significant change in weight. Savage et al [18] reported that subject 2 (S2) with FPLD was heterozygous for a proline-467-leucine (P467L) mutation in *PPARG*, whereas subject 3 (S3) with FPLD was heterozygous for a valine-290-methionine (V290M) mutation in *PPARG*. The metabolic impact of rosiglitazone was much more striking in S2, in whom insulin sensitivity and HbA_{1c} were both normalized, whereas S3 remained severely insulin resistant and exhibited little change in HbA_{1c}. Fat mass was increased by 3.5 kg in S2 and was increased by 4.0 kg in S3 after rosiglitazone treatment for 6 months, indicating that rosiglitazone induced adipocyte differentiation in both cases. Adiponectin level was low before treatment and showed slight increase in both cases. Owen et al [23] also reported no clear advantages in treating patients with FPLD caused by a mutation in the *LMNA* gene (R482W) with rosiglitazone despite increases in subcutaneous adipose tissue. The effects of TZDs on glycemic control, body weight, and adiponectin thus appear to vary in patients with various forms of FPLD [14,18,22-24].

We also measured changes in fat and lean mass during pioglitazone treatment by DEXA scan. As shown in Table 4, fat mass increased by 2.2kg, whereas lean mass increased by 0.7 kg during pioglitazone treatment. Table 4 also shows that subcutaneous fat in the abdomen increased during pioglitazone treatment, consistent with a previous report [7]. Pioglitazone induced increase in fat mass almost equally in the upper limbs, lower limbs, and trunk, although the increase was less in the lower limbs than in the other 2 regions, suggesting a defect in adipocyte differentiation in the lower limbs where fat atrophy exists. Pioglitazone may thus improve glycemic control through adipocyte differentiation from progenitor cells mainly in the upper limbs and trunk [25,26].

Garg [27] has reported that women with Dunnigan-type FPLD have twice the prevalence of diabetes and more than 3 times the prevalence of atherosclerotic vascular disease as men. The mother of our patient with partial lipodystrophy had diabetes and died of cerebral infarction. Regular evaluation for atherosclerosis will therefore be required in this patient.

In conclusion, we have described the phenotype of a case of FPLD case of Asian origin, which differs from that of FPLD cases of European origin. As there were no mutations in the causative genes of *LMNA*, *PPARG*, *AKT2*, caveolin-1, and *PPARG4* promoter, known to be associated with FPLD, it may be that a novel gene is involved in this case. More FPLD cases of Asian origin will need to be examined to determine the clinical features, phenotype, and genotype of Asian cases of FPLD.

Acknowledgment

We thank Dr Takashi Shiokawa (Tanita, Tokyo, Japan) for providing us with the DEXA data of 55 healthy women between the ages of 40 and 49 years.

References

[1] Garg A. Acquired and inherited lipodystrophies. N Eng J Med 2004;350:1220-34.
[2] Agarwal AK, Garg A. Genetic disorders of adipose tissue development, differentiation and death. Annu Rev Genomics Hum Genet 2006;7:175-99.
[3] Agarwal AK, Garg A. Genetic basis of lipodystrophies and management of metabolic complications. Annu Rev Med 2006;57:297-311.
[4] Ebihara K, Kusakabe T, Hirata M, Masuzaki H, Miyanaga F, Kobayashi N, et al. Efficacy and safety of leptin-replacement therapy and possible mechanisms of leptin actions in patients with generalized lipodystrophy. J Clin Endocrinol Metab 2007;92:532-41.
[5] Dunnigan MG, Cochrane MA, Kelly A, Scott JW. Familial lipoatrophic diabetes with Dominant transmission. Q J Med 1974; 169:33-48.
[6] Arita Y, Kihara S, Ouchi Nm Takahashi M, Maeda K, Miyagawa J, Hotta K, et al. Paradoxical decrease of an adipose-specific protein, adiponectin, in obesity. Biochem Biophys Res Commun 1999;257: 79-83.
[7] Akazawa S, Kawasaki E, Sun F, Eguchi K, Ito M. Efficacy of troglitazone on body fat distribution type 2 diabetes. Diabetes Care 2000;23:1067-71.
[8] Sandre-Giovannoli AD, Chaouch M, Kozlov S, Vallat JM, Tazir M, Kassouri N, et al. Homozygous defects in *LMNA*, encoding lamin A/C nuclear-envelope proteins, cause autosomal recessive axonal neuropathy

in human (Charcot-Marie-Tooth disorder type 2) and mouse. Am J Hum Genet 2002;70:726-36.

[9] Elbrecht A, Chen Y, Cullinan CA, Hayers N, Leibowitz MD, Moller DE, et al. Molecular cloning, expression and characterization of Human peroxisome proliferator activated receptors r1 and r2. Biochem Biophys Res Commun 1996;224:431-7.

[10] George S, Rochford JJ, Wolfrum C, Gray SL, Schinner S, Wilson JC, et al. Family with severe insulin resistance and diabetes due to a mutation in *AKT2*. Science 2004;304:1325-8.

[11] Kim CA, Delepine M, Boutet E, Mourabit HE, Lay SL, Meier M, et al. Association of a homozygous nonsense caveolin-1 mutation with Berardinelli-Seip congenital lipodystrophy. J Clin Endocrinol Metab 2008;93:1129-34.

[12] Shali KA, Cao H, Knoers N, Hermus R, Tack CJ, Hegele RA. A single-base mutation in the peroxisome proliferator–activated receptor G4 promotor associated with altered in vitro expression and partial lipodystrophy. J Clin Endocrinol Metab 2004;89:5655-60.

[13] Johansen K, Rasmussen MH, KJEMS LL, Astrup A. An unusual type of familial lipodystrophy. J Clin Endocrinol Metab 1995;80:1106-18.

[14] Sleilati GG, Leff T, Bonnett JW, Hegele R. Efficacy and safety of pioglitazone in treatment of a patient with an atypical lipodystrophy syndrome. Endocri Pract 2007;13:656-61.

[15] Cao H, Alston L, Rushman J, Hegele RA. Heterozygous CAVI frameshift mutation (MIM601047) in patients with atypical partial lipodystrophy and hypertriglyceridemia. Lipids in Heath and Disease 2008;7:3.

[16] Garg A, Agawal AK. Caveolin-1: a new locus for human lipodystrophy. J Clin Endocrinol Metab 2008;93(4):1183-5.

[17] Shackleton S, Lloyd DJ, Jackson SNJm Evans R, Niermeijer MF, Singh BM, Schmidt H, et al. *LMNA*, encoding lamin A/C, is mutated in partial lipodystrophy. Nat Genet 2000;24:153-6.

[18] Savage DB, Tan GD, Acerini CL, Jebb SA, Agostini M, Gurnell M, et al. Human metabolic syndrome resulting from dominant-negative mutations in the nuclear receptor peroxisome proliferator–activated receptor–G. Diabetes 2003;52:910-7.

[19] Hegele RA, Cao H, Frankowski C, Mathews S, Leff T. *PPARG* F388L, a transactivation-deficient mutant, in familial partial lipodystrophy. Diabetes 2002;51:3586-90.

[20] Agarwal AK, Grag AA. Novel heterozygous mutation in peroxisome proliferator–activated receptor–G gene in a patient with familial partial lipodystrophy. J Clin Endocrinol Metab 2002;87:408-11.

[21] Kadowaki T, Kadowaki H, Taylor SI. A nonsense mutation causing decreased levels of insulin receptor mRNA: detection by a simplified technique for direct sequencing of genomic DNA amplified by the polymerase chain reaction. ProcNatlAcadSciUSA 1990;87:658-62.

[22] Arioglu EA, Duncan-Morin J, Sebring N, Rother KI, Gottlieb N, Hoofnagle AE, et al. Efficacy and safety of troglitazone in the treatment of lipodystrophy syndromes. Ann Intern Med 2000;133: 263-74.

[23] Owen KR, Donohoe M, Ellard S, Hattersley AT. Response to treatment with rosiglitazone in familial partial lipodystrophy due to a mutation in the *LMNA* gene. Diabet Med 2003;20:823-7.

[24] Ludtke A, Heckt K, Geneschel J, Mehnert H, Spuler S, Worman J, et al. Long-term treatment experience in a subject with Dunnigan-type familial partial lipodystrophy: efficacy of rosiglitazone. Diabet Med 2005;22:1611-3.

[25] Lewis GF, Carpentier A, Adeli K, Glacca A. Disordered fat storage and mobilization in the pathogenesis of insulin resistance and type 2 diabetes. Endocrine Reviews 2002;23:201-29.

[26] Smith SA. Central role of the adipocyte in the insulin-sensitising and cardiovascular risk modifying action of the thiazolidinediones. Biochime 2003;85:1219-30.

[27] Garg A. Gender differences in the prevalence of metabolic complications in familial partial lipodystrophy (Dunnigan variety). J Clin Endocrinol Metab 2000;85:1776-82.

ARTICLE IN PRESS

Available online at www.sciencedirect.com

ScienceDirect

Metabolism Clinical and Experimental xx (2010) xxx–xxx

Metabolism
Clinical and Experimental

www.metabolismjournal.com

Adipose tissue–specific dysregulation of angiotensinogen by oxidative stress in obesity

Sadanori Okada[a,b,1], Chisayo Kozuka[a,1], Hiroaki Masuzaki[a,*], Shintaro Yasue[a], Takako Ishii-Yonemoto[a], Tomohiro Tanaka[a], Yuji Yamamoto[a], Michio Noguchi[a], Toru Kusakabe[a], Tsutomu Tomita[a], Junji Fujikura[a], Ken Ebihara[a], Kiminori Hosoda[a], Hiroshi Sakaue[c], Hiroyuki Kobori[d], Mira Ham[e], Yun Sok Lee[e], Jae Bum Kim[e], Yoshihiko Saito[b], Kazuwa Nakao[a]

[a]*Department of Medicine and Clinical Science, Kyoto University Graduate School of Medicine, Kyoto 606-8507, Japan*
[b]*First Department of Internal Medicine, Nara Medical University, Kashihara 634-8522, Japan*
[c]*Department of Nutrition and Metabolism, Institute of Health Biosciences, The University of Tokushima Graduate School, Tokushima 770-8503, Japan*
[d]*Departments of Medicine and Physiology, and Hypertension and Renal Center of Excellence, Tulane University Health Sciences Center, New Orleans, LA 70112-2699, USA*
[e]*Institute of Molecular Biology and Genetics, Seoul National University, Seoul 110-744, South Korea*

Received 27 August 2009; accepted 18 November 2009

Abstract

Adipose tissue expresses all components of the renin-angiotensin system including angiotensinogen (AGT). Recent studies have highlighted a potential role of AGT in adipose tissue function and homeostasis. However, some controversies surround the regulatory mechanisms of AGT in obese adipose tissue. In this context, we here demonstrated that the AGT messenger RNA (mRNA) level in human subcutaneous adipose tissue was significantly reduced in obese subjects as compared with nonobese subjects. Adipose tissue AGT mRNA level in obese mice was also lower as compared with their lean littermates; however, the hepatic AGT mRNA level remained unchanged. When 3T3-L1 adipocytes were cultured for a long period, the adipocytes became hypertrophic with a marked increase in the production of reactive oxygen species. Expression and secretion of AGT continued to decrease during the course of adipocyte hypertrophy. Treatment of the 3T3-L1 and primary adipocytes with reactive oxygen species (hydrogen peroxide) or tumor necrosis factor α caused a significant decrease in the expression and secretion of AGT. On the other hand, treatment with the antioxidant *N*-acetyl cysteine suppressed the decrease in the expression and secretion of AGT in the hypertrophied 3T3-L1 adipocytes. Finally, treatment of obese *db/db* mice with *N*-acetyl cysteine augmented the expression of AGT in the adipose tissue, but not in the liver. The present study demonstrates for the first time that oxidative stress dysregulates AGT in obese adipose tissue, providing a novel insight into the adipose tissue–specific interaction between the regulation of AGT and oxidative stress in the pathophysiology of obesity.

1. Introduction

Overactivity of the systemic renin-angiotensin system (RAS) is one of the central mechanisms for obesity-related metabolic disorders [1,2]. Notably, the major components of the RAS are expressed in various tissues including the heart, blood vessels, adipose tissue, and brain [3]; these comprise tissue RAS. A series of products are produced locally from

The authors of this manuscript have nothing to declare.

Institutional approval: The human study was approved by the ethics committee for human research of the Kyoto University Graduate School of Medicine (2004, no. 553). Written informed consent was obtained from all subjects prior to the study. All animal experimental procedures were approved by the Kyoto University Graduate School of Medicine Animal Research Committee and the Seoul National University Animal Experiment Ethics Committee.

* Corresponding author. Division of Endocrinology and Metabolism, Second Department of Internal Medicine, Faculty of Medicine, University of the Ryukyus, Okinawa 903-0215, Japan. Tel.: +81 98 895 1145; fax: +81 98 895 1415.
E-mail address: hiroaki@med.u-ryukyu.ac.jp (H. Masuzaki).

[1] Sadanori Okada and Chisayo Kozuka contributed equally to this work.

0026-0495/$ – see front matter © 2010 Elsevier Inc. All rights reserved.
doi:10.1016/j.metabol.2009.11.016

angiotensinogen (AGT), the unique precursor of angiotensin peptides, and play a critical role in cardiovascular homeostasis [3,4].

Although AGT is produced mainly by the liver, adipose tissue is also considered as a source of AGT production [5]. In agreement with this notion, the adipose tissue expresses all components of the RAS, including AGT, renin, angiotensin I–converting enzyme, and angiotensin II type 1 receptor, in humans and rodents [6,7]. A previous study has demonstrated that AGT-deficient mice are low in blood pressure and body fat mass [8]. Moreover, adipocyte-specific transgenic overexpression of AGT on an AGT-deficient background was shown to augment plasma AGT level and rescue hypotension and leanness [9]. These results indicate that adipose tissue–derived AGT does contribute to the circulating AGT level and adipogenesis.

In rodent experiments, the AGT messenger RNA (mRNA) level in white adipose tissue has been shown to be regulated by the nutritional status; however, that in the liver was independent of the nutritional status [10,11]. In human cross-sectional studies, the AGT mRNA level in adipose tissue was shown to be higher in obese subjects [6,12]. On the other hand, another study reported that the AGT mRNA level in adipose tissue was significantly lower in obese individuals [13]. Elevation of AGT expression in adipose tissue in obese individuals thus remains controversial [14].

Several studies have shown that increased oxidative stress is a manifestation of obesity-related metabolic derangement [15-17]. In fact, in humans, oxidative stress is critically associated with atherosclerosis, hypertension, and diabetes mellitus [18,19]. Oxidative stress is also related with the RAS. Angiotensin II is a potent inducer of reactive oxygen species (ROS) in a variety of tissues [20-22]. In the liver and kidney, increased ROS has been reported to increase AGT gene expression [23-26]. Also in obese adipose tissue, generation of ROS is exaggerated and is involved in adipose tissue dysfunction [17,27]. However, whether increased ROS may affect adipose AGT production remains to be elucidated.

In the present study, we demonstrated that the AGT mRNA level was reduced in obese adipose tissue in humans and mice and in hypertrophied 3T3-L1 adipocytes. In this context, we tested the hypothesis that increased oxidative stress would modulate AGT in obese adipose tissue.

2. Materials and methods

2.1. Subcutaneous abdominal adipose tissue biopsies in human subjects

The present study was performed according to the Declaration of Helsinki and approved by the Ethical Committee on Human Research of Kyoto University Graduate School of Medicine (2004, no. 553). Written informed consent was obtained from all subjects before the study.

Subcutaneous abdominal adipose tissue biopsies were obtained from 46 Japanese subjects (24 men and 22 women; age [mean ± SD], 46 ± 2.1 years). The body mass index (BMI) of the subjects ranged from 19 to 52 (mean ± SD, 30 ± 1.6) kg/m^2. All subjects had been on stable therapy with lipid-lowering, antihypertensive, or hypoglycemic agents for at least 1 month before admission and continued with the same doses throughout the study period. Patients who received angiotensin I–converting enzyme inhibitors, angiotensin II receptor blockers, and steroid-related drugs were carefully excluded. For the study, subcutaneous abdominal adipose depots of the study subjects were excised from the periumbilical region under local anesthesia. The samples were immediately frozen in liquid nitrogen and stored at −80°C until use.

2.2. Mouse experiments

Male *ob/ob* mice (age, 12 weeks) were purchased from Oriental BioService (Kyoto, Japan) and housed in the animal facility of Kyoto University. Male *db/db* mice (age, 10 weeks) were purchased from Japan SLC (Hamamatsu, Japan) and housed in Seoul National University. The mice were allowed free access to food and water. For in vivo antioxidant treatment, the *db/db* mice were injected with *N*-acetyl cysteine (NAC; 150 mg/kg body weight; Sigma-Aldrich Japan, Tokyo, Japan) or the vehicle (phosphate-buffered saline) into the peritoneal cavity once daily for 1 week. All experimental procedures were approved by the Kyoto University Graduate School of Medicine Animal Research Committee and the Seoul National University Animal Experiment Ethics Committee.

2.3. Cell culture and isolation of primary adipocytes

3T3-L1 fibroblasts were cultured and differentiated into adipocytes as described previously [28]. Briefly, the 2-day postconfluent cells (designated as day 0) were incubated for 2 days with 10% fetal bovine serum (FBS)/Dulbecco modified Eagle medium (DMEM), 0.5 mmol/L 3-isobutyl-1-methylxanthine, 0.25 μmol/L dexamethasone, and 1 μg/mL insulin. The cells were then incubated for 2 days in 10% FBS/DMEM with insulin and, thereafter, incubated in 10% FBS/DMEM that was changed on every alternate day. Oil red O staining was performed as described [29].

Primary adipocytes were isolated from epididymal fat pads of 9-week-old male C57BL/6J mice (purchased from Oriental BioService, Kyoto, Japan). Epididymal fat pads were harvested, minced into 2- to 3-mm pieces, and digested using 0.8 mg/mL collagenase (Sigma-Aldrich Japan) in DMEM for 30 minutes at 37°C in a shaking water bath. After the digestion with collagenase, cells were filtered through a 250-μm nylon filter and centrifuged at 1000 rpm for 30 seconds. The suspended mature adipocytes were separated from the pelleted stromovascular fraction and washed 3 times in DMEM for experiments.